Anthropogenic impact of rare earth elements on groundwater and surface water in the watershed of the largest freshwater lake in China

Haiyan Liu, Huaming Guo, Olivier Pourret, Zhen Wang

Anthropogenic impact of rare earth elements on groundwater and surface water in the watershed of the largest freshwater lake in China

Haiyan Liu [1, 2, *], Huaming Guo [3], Olivier Pourret [4], Zhen Wang[1, 2]

1 State Key Laboratory of Nuclear Resources and Environment, East China University of Technology, Nanchang 330013, PR China

2 Jiangxi Provincial Key Laboratory of Genesis and Remediation of Groundwater Pollution and School of Water Resources and Environmental Engineering, East China University of Technology, Nanchang 330013, PR China

3 MWR Key Laboratory of Groundwater Conservation and School of Water Resources and Environment, China University of Geosciences (Beijing), Beijing 100083, PR China

4 UniLaSalle, AGHYLE, Beauvais, France

*** Corresponding author:**

Dr. Haiyan Liu: hy_liu@ecut.edu.cn

418 Guanglan Road, Jingkai District, Nanchang, P. R. China **(H. Liu)**;

Tel.: +86-1881-3181-419

Fax: +86-0791-8389-8197

Abstract: Limited knowledge exists regarding the potential risks associated with anthropogenic release of rare earth elements (REEs) in the environment. This study aimed to investigate REE signatures in the watershed Poyang Lake, the largest freshwater lake in China. Samples of surface water, wastewater, and groundwater were collected from five rivers discharging into the lake. Results revealed wastewater from wastewater treatment plants contained total REE concentrations from 231 to 904 μg/L, exceeding those found in surface water (0.4 to 1.3 μg/L) and groundwater (0.5 to 416 μg/L). Samples with elevated REE were found in Ca-Mg-Cl/SO_4 type waters and exhibited an ^{18}O-D deviation from local meteoric water line. Wastewater exhibited a higher positive Gd anomaly compared to surface water and groundwater, attributed to anthropogenic input of Gd (Gd_{anth}). The determined Gd_{anth} concentration ranged from 0.04 to 0.21 μg/L, and from 0.06 to 0.37 μg/L, accounting for 4% to 21% and 49% to 84% of total Gd concentrations in groundwater and surface water, respectively. Gd_{anth} concentration in wastewater (0.19 to 0.43 μg/L) remained constant in effluent after wastewater treatment. Surface water displayed relatively complex normalized REE patterns influenced by anthropogenic activities and natural processes (weathering and complexation), while groundwater exhibited heavy REEs enrichment, due to carbonate solution complexation. Additionally, Gd_{anth} concentration showed a positive correlation with ΣREE, Pb, Ni, and Co concentrations in groundwater, indicating a good pollution tracing potential. Health risk assessment using the hazard quotient (HQ) suggested higher HQ_{Gd} values in groundwater compared to surface water. Residents in the eastern part of Poyang Lake were found to face higher risks associated with Gd in groundwater

compared to the western part, with infants and children at greater risk than adult males and females. These findings offer valuable insights into environmental behavior and health risks of REEs in aquatic systems impacted by human activities.

Keywords: Lanthanides; Water environment; Gd anomaly; Health risk; Human activity

1. Introduction

Rare earth elements (REEs) constitute a group of critical elements usually including 15 lanthanides from lanthanum (La) to lutetium (Lu) plus yttrium (Y) and scandium (Sc). These elements are further categorized into light REEs (LREEs: La to Nd), middle REEs (MREEs: Sm to Dy) and heavy REEs (HREEs: Ho to Lu) based on atomic weight and ionic radii (Haskin and Haskin, 1966). Their uniform valence shell configurations underpin their cohesive behavior in natural environments, manifesting in their co-occurrence in geomatrices and responsiveness to variations in pH, redox conditions, and solution complexations (Guo et al., 2010; Noack et al., 2014). Consequently, REEs have been widely used as a proxy for understanding geochemical processes in various aquatic systems (Rabiet et al., 2009; Pourret et al., 2010; Hatje et al., 2016; Wilkin et al., 2021).

Naturally, REEs primarily enter surface water and groundwater mainly through the weathering of source rock (Nesbitt, 1979; Smedley,1991; Sholkovitz, 1993; Gaillardet et al., 2005). Both primary and secondary minerals serve as sources of REEs for surface water and groundwater, with REE concentration and fractionation in aqueous media largely influenced by interactions with minerals bearing REEs (Munemoto et al., 2015). Various processes, including redox reactions, solution complexation, and adsorption/desorption, could further modify REE signatures (Verplanck, 2013). Conversely, REEs find extensive applications in modern society across multiple sectors, including green energy production (Golroudbary et al., 2022), agricultural fertilization (Hu et al., 2006), medical diagnosis (Bau and Dulski, 1996),

petroleum industry (Doronin et al., 2015), and livestock management (Liu et al., 2023) owing to their unique functions such as spectroscopic and magnetic properties, as well as their high practical value. The widespread use of REEs has led to an increased release of these elements into the environment (Hatje et al., 2016; González et al., 2015; Junqueira et al., 2024). Indeed, accumulations of anthropogenic REEs in surface water (Nozaki et al., 2000; Kulaksiz and Bau, 2013; Kreitsmann and Bau, 2023) and groundwater (Knappe et al., 2005; Johannesson et al., 2017) have been observed. Among them, anthropogenic gadolinium (Gd) has been detected worldwide, primarily due to its widespread use in magnetic resonance imaging (MRI) (Nozaki et al., 2000; Kulaksiz and Bau, 2013; Hatje et al., 2016; Wang et al., 2021; Liu et al., 2022c).

The ubiquitous presence of anthropogenic Gd in water can be attributed to its extensive use in MRI as a contrast agent, typically in the form of an organically chelated compound (Caravan et al., 1999). Although the free ion of Gd is highly toxic, the chelated species is generally considered safe for ingestion by humans (Ramalho et al., 2017). However, concerns persist regarding the potential carcinogenic effects of Gd salts, although this has yet to be conclusively confirmed (Takahashi et al., 2005). Organic chelating forms of Gd are known for their stability, making them effective tracers of wastewater pollution in aquatic ecosystems (Port et al., 2008; Migaszewski and Gałuszka, 2015; De Paula Marteleto and Enzweiler, 2021). Studies have investigated various aspects related to anthropogenic Gd, including the infiltration of surface water into groundwater (Bichler et al., 2016), leakage detection of wastewater into surface water (Brünjes et al., 2016), and groundwater pollution remediation efforts

(Wilkin et al., 2021). Positive Gd anomaly has been used to discriminate groundwater pollution by anthropogenic sources (i.e., wastewater sludge application in agriculture, industrial activity, and wastewater treatment plants (WWTP)) from natural sources (Petelet-Giraud et al., 2009). For example, the proportion of anthropogenic Gd has been found to correlate with chromium concentrations in river water (Peng, 2020). Furthermore, Barber et al. (2006) highlighted the co-occurrence of pharmaceuticals and anthropogenic Gd in groundwater, particularly in areas characterized by intensive urbanization. These studies suggest that anthropogenic Gd may serve as an effective indicator of various contaminants in aquatic systems affected by human activities.

Concerns regarding the potential health risks associated with anthropogenic Gd and REEs have been raised, because studies have demonstrated that elevated concentrations of REEs resulting from anthropogenic discharges can be toxic to plants and aquatic animals (Adeel et al., 2019; Rue and McKnight, 2021). Various pathways, including ingestion, inhalation, and skin contact, induce human exposures to REEs (Shin et al., 2019; Brouziotis et al., 2022). Toxicological studies have investigated the health effects associated with REE exposure, revealing adverse outcomes from occupational and/or environmental exposures to REEs (Cassee et al., 2011; Pagano et al., 2012). Studies by Zhuang et al. (2017) and Squadrone et al. (2019) explored the accumulations and health risk of REEs in vegetables and marine organisms. Long term consumption of low-dose REE-bearing drinking water could cause significant damage renal system (Vergauwen et al., 2018), immune system (Pagano et al., 2015a), and induce nephrogenic fibrosis (Gwenzi et al., 2018). For instance, intake of REEs at

concentration ranging from 2 to 20 mg/L has been suggested to lead to bone alternation (Chen and Zhu, 2008). Renal toxicity has also been reported from iatrogenic exposure to Gd used as a contrast agent in MRI (Thomsen, 2006; Bernstein et al., 2012). A recent study demonstrated that the production of reactive oxygen species can be altered by REEs once entering human body, causing DNA and cell damage, cell death, and presenting higher toxicity to cancer cells (Brouziotis et al., 2022). However, comprehensive understanding of the potential environmental and health risks associated with REEs remains incomplete, and data linking residents health conditions to dissolved REE exposure remain limited (Pagano et al., 2015b), despite REEs being recognized as emerging contaminants. Therefore, the objectives of this study are to (i) investigate REE concentrations in surface water and groundwater and their controlling factors, (ii) assess the potential traceability of anthropogenic REEs in the aqueous environments, and (iii) evaluate the human health risks associated with anthropogenic REEs in surface water and groundwater.

2. Materials and methods

2.1 Study area

The Poyang Lake is located in the north of Jiangxi Province at longitudes of 115º49′ – 116º46′ and latitudes of 28º24′ – 29º46′(Fig. 1). It is the largest freshwater lake in China with maximum inundation area >3000 km^2 (Feng et al., 2013). It receives water and sediment primarily from five major rivers, namely, Fu, Rao, Xin, Ganjiang, and Xiushui, and drains into the Yangtze River to the north (Fig.1a). The water recharge

from the five tributaries and discharge into Yangtze River is highly dependent on season, dominating in rainy season from March to September (Wang et al., 2023). Among the five rivers, the Ganjiang River is the largest one. It runs across Nanchang city, the capital city of Jiangxi Province with a total length of 766 km and a mean annual discharge of 2130 m^3/s, which occupies 55% of the total flow into Poyang Lake (Zhang et al., 2017). Topographically, the Poyang Lake is surrounded by small mountains, and the central areas are characterized by hills and valleys. The elevations generally slope from south-east to north-west (Zheng et al., 2021). An alluvial plain is distributed towards the north related to the five rivers. Different land-use including forestry, plowland, open water, and mining and industry, accounting for 58%, 21%, 9%, and 6% of total area, respectively (Chu, 2022). The intense aquatic vegetations make the Poyang Lake basin a natural ecosystem for biodiversity.

The basement of Poyang Lake is composed of metamorphic, clastic, carbonate, and magmatic rocks (Zhan et al., 2016). The metamorphic rocks are intensely fractured by a weathered layer of slate, phyllite, and metasandstone. The clastic rocks are represented by sand shale stone and conglomerates of ages from Paleozoic to Mesozoic. The carbonatic rocks are dominated by limestone and dolomite, and magmatic rocks are mainly granite (Zhang, 1986). Groundwater resources are relatively abundant in the study area due to a fractured basin structure controlled by 13 geological faults (Zhan et al., 2016). Unconfined groundwater around the lake is hosted by Quaternary porous aquifers in unconsolidated sediments, fissured bedrock aquifers, karst aquifers, and pore-fissure aquifers in clastic rocks (Fig. 1b) (Mao et al., 2021). The Quaternary

porous aquifer, the main aquifer occurring along the margins of the lake, has depths of 20-50 m and consists of unconsolidated fluvial and lacustrine sediments, with a lithology of loam, medium sand, lateritic gravel, sandy gravel, reticulated laterite, and organic clay (Shvartsev et al., 2016). Groundwater is mainly recharged by precipitation and surface water infiltration, mountain discharges in spring, and lateral flow in lateritic plain aquifers. Groundwater flow directions follow a decreasing trend of elevations, generally from the hill and mountain areas to the lake and alluvial plain area (Fig. 1c). Due to hydrological exchanges with the five rivers and Yangtze River, groundwater regime is affected by surface runoff (Chu, 2022). Water chemistry is influenced by natural processes and anthropogenic activities. Weathering of minerals contained in earth crusts contributes compositions to watershed including REEs (Meng, 2007). Possible sources of REEs may also be related to mining activities, which occur frequently along the five rivers.

2.2 Sampling

Eighty-two water samples were collected from the study area in July 2021, including 54 groundwater samples, 23 surface water samples, and 5 wastewater samples. All sampling locations are shown in Fig. 1a. Groundwater was sampled from local wells used for drinking water supply or irrigation, with sampling depths ranging between 6 m and 50 m. The sampled wells were generally pumped for >20 min before sampling to ensure the groundwater came from the aquifer rather than from the borehole filling. Surface water was sampled along rivers at 30 cm – 40 cm below water surface. Among them, 9 were from Rao River, 4 from both Xin River and Ganjiang River, 3 each from

Fu River and Xiushui River. Wastewater was sampled from influents and effluents of 3 wastewater treatment plants (WWTP, labeled as W-A, W-B, and W-C in Fig.1a). All water samples were filtered by 0.22 μm cellulose acetate membranes. At each sampling site, 50 mL sample were filled in high-density polyethylene (HDPE) bottles and acidified by HNO_3 (ultrapure quality) to pH <2 for cation and trace element analysis. Other portions of 30 mL filtered water were sampled in HDPE bottles but without acidification for anion analysis. Another 10 mL water was sampled in a centrifuge tube without acidification for stable hydrogen and oxygen isotope analysis. For REE analysis, about 500 mL membrane-filtered water was sampled in HDPE bottles and acidified by using HNO_3. All samples were preserved in a cryobox and transported to the laboratory as soon as possible for analysis.

2.3 Analysis

During sampling, redox potential (ORP), electrical conductivity, temperature, and pH were measured using a HI 9828 portable multi-meter (HANNA, Woonsocket, RI, USA). These parameters were recorded by immersing the monitoring probe in flowing water. The ORP data were converted into standard hydrogen potentials (Eh values) using the website tool by Wolkersdorfer (https://www.wolkersdorfer.info/en/redoxprobes.html). Alkalinity of water samples was determined in-situ with a Model 16,900 digital titrator (HACH, Loveland, USA). Total Fe, Fe^{2+}, S^{2-}, and NH_4^+-N were measured by a portable UV/VIS spectrophotometer (HACH, DR2800). In the laboratory, cations and metal ions were detected by inductively coupled plasma optical emission spectrometry (ICP-OES

iCAP6300, Thermo Fisher Scientific, Waltham, USA). Trace elements (i.e., Pb, Co, Ni, etc) were determined by inductively coupled plasma mass spectrometry (ICP-MS 7500C, Agilent Technologies, Santa Clara, USA). Anions were quantified using an ion chromatography system (ICS2000, Dionex, Thermo Fisher Scientific, Waltham, USA). The analytical results were verified with replicate samples and standard solutions, ensuring the ionic charge balance error to be better than 5%. Stable isotopes (^{18}O and D) were determined using a wavelength scanning optical cavity ring-down spectrometer (Picarro L2120-I) with accuracy better than 0.1‰ and 1‰, respectively.

Concentrations of REEs were quantified using two different single-collector inductively coupled plasma sector field mass spectrometry instruments (ICP-SFMS ELEMENT XR and ELEMENT 2, Thermo Fisher Scientific, Bremen, Germany) following the method published by Rodushkin et al. (2018). The specific procedures were detailed in Liu et al. (2022a). Briefly, REEs in water were preconcentrated with a cation exchange resin (AG 50 W-X8, 200 to 400 dry mesh size, Bio-Rad laboratory AB, Solna, Sweden). This was performed with a 2 mL low-density polyethylene (LDPE) column being equipped with the resins, which was conditioned by loading sequentially 4 mL of 14 mol/L HNO_3 (AR), 8 mL deionized water, and 4 mL of 9.5 mol/L HCl (AR). Then, 400 mL water sample was rinsed through the column, and 4 mL of 0.5 mol/L HCl was used to elute the column. As a result, the REEs were preconcentrated by 100-fold before being analyzed by ICP-SFMS. During analysis, different resolution modes were set up for monitoring different REEs as proposed by Wilkin et al. (2021). Generally, isotopes ^{163}Dy, ^{151}Eu, ^{165}Ho, ^{146}Nd, ^{147}Sm, and ^{172}Yb were measured under a medium

resolution mode (MR, m/Δm approximately 5400), while isotopes ^{140}Ce, ^{166}Er, ^{157}Gd, ^{139}La, ^{175}Lu, ^{141}Pr, ^{159}Tb, and ^{169}Tm were measured under a high-resolution mode (HR, m/Δm approximately 12,000). Isotopes ^{151}Eu and ^{153}Eu are known to be affected by BaO^+ interference. To correct for this interference, a correction measure was established with known Ba concentration in solutions that run through the ICP-SFMS using the peak area of the Eu isotopes. Meanwhile, internal standards (i.e., Rh, In, and Re) were used to check for the analytical precision. The results yielded REE recovery rates between 92% and 104%, and analytical precision better than 8%.

2.4 Health risk assessment

The human health risk assessment (HHRA) model by USEPA (1989) was used to evaluate the potential impact of REE-contaminated surface water and groundwater on human health (Li et al., 2019; Xiao et al., 2022). Four population ages (i.e., infants (< 6 months), children (7 months to 17 years), adult males and females (> 17 years)), divided based on their different behavior and physiology, were chosen for the estimations. Oral ingestion was considered as the main pathway to exposure. The potential risk was calculated using Eqs. (1) to (3).

$$CDI_i = \frac{C_i \times IR \times EF \times ED}{BW \times AT} \quad \text{Eq. (1)}$$

$$AT = ED \times 365 \quad \text{Eq. (2)}$$

where CDI_i is the chronic daily intake dose of REE (mg/(kg × day)), C_i is the REE concentration in groundwater (mg/L), IR indicates the amount of daily intake of water (L/day), EF denotes the frequency of exposure (days/year), ED is annual exposure

duration (years), BW denotes the mean body weight (kg), and AT is the mean exposure time (days, AT = ED × 365).

$$HQ_i = \frac{CDI_i}{RfD_i} \quad \text{Eq. (3)}$$

where HQ_i represents the potential noncarcinogenic risk of REE, and RfD_i denotes the reference dose of REE through the oral intake route. Corresponding values of relevant parameters used in the model are listed in Table S1. Potential health risk can be classified into three categories according to the HQ values, namely, low health risk with HQ < 1 indicating acceptable non-carcinogenic health risk caused by REE, moderate health risk with HQ between 1 and 4 reflecting increased health risk, and high health risk with HQ > 4 suggesting an unacceptable health risk which will cause obvious adverse effects on human health (USEPA, 2004).

2.5 Modeling approach

REE speciation in waters were calculated by using the hydrogeochemical code PHREEQC version 3.6 (Parkhurst and Appelo, 2013) with the Nagra/PSI database (Hummel et al., 2002). The database was updated by incorporating the stability constants for REE complexation to major anions including CO_3^{2-}, SO_4^{2-}, OH^-, Cl^-, and NO_3^-. Constants for $REE(CO_3)_2^-$ and $REECO_3^+$ were taken from Luo and Byrne (2004), and those for $REESO_4^+$ were taken from Schijf and Byrne (2004). Details on the modelling performance were published previously by Liu et al. (2022).

3. Results

3.1 Hydrochemical characteristics

The hydrochemical parameters of the groundwater samples are presented in Table S2. Groundwater was weakly acidic to neutral with pH values of 4.55 to 7.50 (Fig. 2). The highest average pH value was found in Ganjiang River (5.47~6.62, average 6.24), followed by Xiushui River (5.55~6.65, average 6.08), Rao River (4.55~7.5, average 5.95), Fu River (5.83~6.04, average 5.83), and Xin River (4.82~5.83, average 5.37). The Eh values in groundwater ranged between 42 mV and 614 mV with an average of 418 mV. Relative higher Eh values were observed in Rao River (average 615 mV) and Xin River (average 568 mV), as compared to Fu River (average 482 mV), Ganjiang River (average 520 mV), and Xiushui River (average 463 mV). Total dissolved solids (TDS) ranged from 55 mg/L to 1467 mg/L (average 149 mg/L) and were decreasing from Rao River (average 235 mg/L) > Ganjiang River (average 131 mg/L) > Fu River (average 91 mg/L) > Xiushui River (average 77 mg/L) > Xin River (average 71 mg/L). Based on the average milliequivalent concentrations in groundwater, the major anion abundance followed an order of $Cl^- > HCO_3^- > SO_4^{2-} > NO_3^- > F^-$, and the major cation abundance followed an order of $Ca^{2+} > Mg^{2+} > Na^+ > K^+$ (Fig. 3a).

Surface water samples generally had higher pH values than groundwater, with a range of 6.53 to 9.23 (average 7.09) (Table S3). The pH value in samples collected from Ganjiang River ranged between 6.92 and 9.23 with an average of 8.04, higher than that of Xiushui River (7.15), Xin River (7.07), Rao River (6.83), and Fu River (6.56). TDS values varied from 55 mg/L to 1467 mg/L with an average of 149 mg/L. Higher average TDS values were found in Rao River (235 mg/L) and Ganjiang River (131 mg/L) as

compared to Fu River (91 mg/L), Xiushui River (77 mg/L), and Xin River (71 mg/L) (Fig. 2). Sulfate was the dominant anion in surface water with concentrations ranging from 5 mg/L to 846 mg/L (average 51 mg/L). Concentrations of SO_4^{2-} were generally higher in surface waters from Rao River (5.53 mg/L to 845.93 mg/L, average 113.26 mg/L) compared to the other four rivers. HCO_3^- was the second highest abundant anion (14 mg/L to 58 mg/L, average 23 mg/L), followed by Cl^- (2.1 mg/L to 28.4 mg/L, average 12.3 mg/L) and NO_3^- (3.5 mg/L to 40.9 mg/L, average 9.0 mg/L). Fluoride concentrations were all below 1 mg/L. Cation in surface water was predominated by Ca^{2+} with concentrations ranging from 7.4 mg/L to 247 mg/L (average 22.0 mg/L), followed by K^+ (average 8.8 mg/L), Mg^{2+} (average 7.2 mg/L) and Na^+ (average 3.3 mg/L).

Stable isotopes (D and ^{18}O) compositions are presented in Table S4 and S5. Values of $\delta^{18}O$ and δD ranged between -6.9‰ and -4.3‰, and between -45.4‰ and -26.4‰ in groundwater, respectively. For surface water, $\delta^{18}O$ and δD ranged between -7.4‰ and -5.2‰, and between -46.4‰ and -30.5‰, respectively. Surface water samples were mostly located along the local meteoric water line (LMWL) with a slope of 7.08 for the regression equation, indicating an origin of local precipitation. Groundwater samples were mostly plotted near LMWL in between the surface water samples (Fig. 3b), indicating both precipitation and surface water as sources. Intriguingly, those samples containing relatively higher REE concentrations tended to deviate from LMWL.

3.2 REE concentration and fractionation

Concentrations of dissolved REE in groundwater are compiled in Table S6. Total

312 REEs (ΣREE) concentrations in groundwater ranged between 433 ng/L and 416,030
313 ng/L, averaging 10096 ng/L. The average ΣREE concentrations in groundwater
314 obtained from the five rivers followed an order of Rao River (464 ng/L to 416,030 ng/L,
315 average 37812 ng/L) > Xin River (488 ng/L to 20,977 ng/L ng/L, average 6841 ng/L) >
316 Fu River (528 ng/L to 2544 ng/L ng/L, average 1218 ng/L) > Xiushui River (512 ng/L
317 to 1479 ng/L ng/L, average 977 ng/L) > Ganjiang River (433 ng/L to 858 ng/L ng/L,
318 average 643 ng/L). Upper continental crust (UCC) normalization showed that
319 groundwater samples of Fu River and Ganjiang River exhibited enrichment of HREEs
320 over LREEs. This was suggested by $(Yb/Nd)_{UCC}$ fractionation measures ranging from
321 0.93 to 16.79 (average 4.39) and from 1.52 and 17.10 (average 5.41) in groundwater of
322 Fu River and Ganjiang River, respectively. As many as 42% of groundwater samples
323 from Rao River were found to be enriched in HREEs, and the remaining were enriched
324 in LREEs. Similar fractionations were observed in groundwater from Xin River, with
325 44% of samples being enriched in HREEs. For groundwater samples taken from
326 Xiushui River, HREEs enrichments was generally featured, with $(Yb/Nd)_{UCC}$ of 0.82 to
327 1.78 (average 1.78). Groundwater mostly exhibited negative Ce anomaly with Ce/Ce*
328 value ranging between 0.05 and 1.46 (average 0.59). Positive Gd and La anomalies
329 prevailed in groundwater with average Gd/Gd* and La/La* value of 1.87 and 52.3,
330 respectively (Fig. 4).

331 Lanthanum, Ce, and Gd anomalies were calculated using Eqs. (4) to (6),
332 respectively (Kulaksiz and Bau, 2011).

333 $$La_{anomly} = La/La^* = La_{UCC}/((Pr_{UCC})^3/(Nd_{UCC})^2) \quad \text{Eq. (4)}$$

$$Ce_{anomly} = Ce/Ce^* = Ce_{UCC}/(La_{UCC} \times Pr_{UCC})^{0.5} \quad \text{Eq. (5)}$$

$$Gd_{anomly} = Gd/Gd^* = Gd_{UCC}/(0.33Sm_{UCC} + 0.67Tb_{UCC}) \quad \text{Eq. (6)}$$

where the subscript UCC denotes that REE abundances are normalized by Upper Continental Crust values.

Surface water contained ΣREE concentrations ranging between 399 ng/L and 1823 ng/L with an average of 802 ng/L. Average ΣREE concentrations followed an order of Fu River (895 ng/L, ranging from 713 ng/L to 1000 ng/L) > Rao River (842 ng/L, ranging from 399 ng/L to 1823 ng/L) > Xin River (840 ng/L, ranging from 481 ng/L to 1258 ng/L) > Xiushui River (701 ng/L, ranging from 480 to 824 ng/L) > Ganjiang River (678 ng/L, ranging from 578 to 897 ng/L) (Table S7). Samples from Fu River and Ganjiang River had HREEs-enriched UCC-normalized patterns with $(Yb/Nd)_{UCC}$ >1. While for samples from Rao, Xin River and Xiushui River, both HREEs-enriched and LREE-enrich patterns were observed. All surface water commonly showed negative Ce anomaly with Ce/Ce* value of 0.61 to 1.12 (average 0.8), and positive Gd and La anomalies with a range of 1.44 to 4.53 (average 2.3) and 1.73 to 57.54 (average 13.83) for Gd/Gd* and La/La*, respectively.

Wastewater had ΣREE concentrations in a range of 231 ng/L to 904 ng/L (Table S7). ΣREE concentrations were lower in effluent samples of the wastewater treatment plant (WWTP) as compared to influent samples. ΣREE concentrations in wastewater decreased by 45% and 31% after treatment in the two WWTPs (labeled as A and B in Fig. 1), respectively. UCC-normalized patterns for wastewater samples showed HREEs enrichment characteristic with $(Yb/Nd)_{UCC}$ value of 1.13 to 13.14 (average 6.22).

Moreover, effluent samples had larger $(Yb/Nd)_{UCC}$ value than that of influent samples. Positive Gd anomaly was evident in all wastewater samples with Gd/Gd* values ranging between 21.7 and 387 (average 117) (Fig. 5f).

3.3 REE speciation

Results of REE speciation calculation were shown in Figs. 6 and S8. Free cations (REE^{3+}), carbonate complexes ($REE\text{-}CO_3^+$) and sulfate complexes ($REE\text{-}SO_4^+$) were predicted to be the main REE species in groundwater (Figs. 6a, b, and c). However, the fractionation of the main REE complexes were different in groundwater samples in the reach of the of different rivers. To take Nd for example, Nd^{3+} and $NdCO_3^+$ accounted for 2% to 91% and 1% < to 92%, with average values of 49% and 39% in groundwater samples collected along the bank of Rao River, respectively. The free cations generally dominated REE species in groundwater samples taken from Xin River, with $NdCO_3^+$ accounting for 51% to 98% (average 82%), followed by $REE\text{-}SO_4^+$ which was 1% to 48% (average 17%). For groundwater samples of Fu River, Nd^{3+} and $NdCO_3^+$ were calculated at 29% to 81% (average 63%) and 7% to 56% (average 24%), respectively. $NdSO_4^+$ was calculated at 3% to 25% (average 13%) in groundwater from Fu River. $REE\text{-}CO_3^+$ was the largest fraction in groundwater samples of Ganjiang River, with $NdCO_3^+$ percentage of 2% to 90% (average 64%), and REE^{3+} was the second abundant species with Nd^{3+} occupying 6% to 96% (average 29%). Similar modelling results have been observed in groundwater samples of Xiushui River, in which percentages of $NdCO_3^+$ and Nd^{3+} were 1% to 87% (average 48%) and 10% to 69% (average 36%), respectively. It should be noted that $NdSO_4^+$ made up on average 15% of total Nd in

groundwater obtained from Xiushui River.

REE speciation in surface water samples was dominated by REE^{3+}, $REE\text{-}CO_3^{+}$ and $REE\text{-}SO_4^{+}$ (Figs. 6d, e, and f). For example, Nd^{3+}, $NdCO_3^{+}$ and $REE\text{-}SO_4^{+}$ accounted for 4% to 72%, 1% to 92%, and 1% to 66%, with average values of 33%, 33%, and 25% for groundwater samples collected from Rao River, respectively. Fractions of $REE\text{-}CO_3^{+}$ and REE^{3+} larger than $REE\text{-}SO_4^{+}$ were observed in groundwater samples taken from Xin River, i.e., $NdCO_3^{+}$ accounted for 46% to 92% (average 66%), and Nd^{3+} accounted for 3% to 38% (average 23%) as compared to $NdSO_4^{+}$ accounting for 1%< to 14% (average 8%). Results of REE modelling using groundwater samples of Fu River showed that $NdCO_3^{+}$ and Nd^{3+} occupied 34% to 53% and 40% to 52%, respectively. For surface water obtained from Ganjiang River and Xiushui River, $REE\text{-}CO_3^{+}$ was the dominant species, followed by REE^{3+}. Specifically, average proportion of $NdCO_3^{+}$ was 76% (52% to 86%) and 78% (62% to 87%), and the average proportion of Nd^{3+} was 16% and 6%, respectively. Appreciable fraction of $REE(CO_3)_2^{-}$ was only found in a few samples of Ganjiang River. However, the proportion of hydroxyl complexes ($REE\text{-}(OH)_n^{(3-n)+}$) increased with increasing REE atomic numbers in both surface water and groundwater (Fig. S8).

4. Discussion

4.1 Control on REE concentrations

Figure 7 shows a comparison of normalized REE patterns for surface water samples with those of other rivers worldwide. The surface water in the Poyang Lake

basin generally showed higher REE concentrations than the values found for the Mississippi (Shiller, 2002), Indus, Ohio (Goldstein and Jacobsen, 1988), and Pearl (Ma and Wang, 2023), Xijiang (Xu and Han, 2009) and Minjiang (Zhu et al., 2018), but lower REE concentrations than those of Amazon (Barroux et al., 2006), YangZe (Li et al., 2005; Liu et al., 2022c), Yellow (He et al., 2005) and Jiulongjiang rivers (Jin et al., 2010). Surface water from the study area contained generally higher REE concentrations than those of some major rivers (i.e., Pearl, Xijiang, and Minjiang Rivers) in southern China. Relatively higher concentrations of La and lower higher concentrations of Ce than other REEs were found in surface waters. This was like results published by Meng and Ji (2007) which studied REE geochemistry upstream of Ganjiang River.

A previous study showed that groundwater from Ganjiang River basin had average ΣREE concentrations of 635 ng/L (Liu et al., 2022b), similar to the value of this study. Compared to groundwaters from other parts of China including North China Plain (65 ng/L to 164 ng/L, average 97 ng/L) (Liu et al., 2016), Hetao basin (40 ng/L to 500 ng/L, average 163 ng/L) (Guo et al., 2010), and Datong basin (72 ng/L to 334 ng/L, average 202 ng/L) (Xie et al., 2012), groundwater showed higher ΣREE concentrations in this study. Concentrations of REEs in the groundwater of North China Plain, Hetao basin, and Datong basin were mainly attributed to geogenic origin, and anthropogenic disruptions in REE (bio) geochemical cycles were not discussed (Libralato et al., 2023).

Generally, REEs in water were derived from weathering of earth crust rocks (Aubert et al., 2001; Ma et al., 2023) and anthropogenic discharges (Bau and Dulski,

1996; Rabiet et al., 2009; Zhang et al., 2019) in this study. Upon weathering, REEs were mobilized from solid phases via water-rock interactions and were transported to aquatic systems. These processes have been shown to result in low dissolved REE concentrations in rivers, because REEs were mainly bound to particulate matter (Han and Liu, 2006; Meng, 2007; Ma et al., 2023). Compared to some important rivers worldwide, the rivers in Poyang Lake basin generally contained higher REE concentrations (Fig. 7). The positive Gd and La anomalies indicated anthropogenic input of REEs into rivers. Studies showed that human activities, such as agricultural practices, contribute REE to rivers entering lakes because of surface runoff, leading to higher REE concentrations than unaffected rivers (Möller et al., 2002; Jiang et al., 2022). Under the conditions that farmland is widely distributed around the Poyang Lake, the REEs that were originated from phosphate fertilizers or WWTP sludges were released into the five adjacent rivers when they flow across the agricultural land-use areas (Pang et al., 2002; Hu et al., 2006; Tang et al., 2020). Wastewater and domestic sewage discharges contribute REEs, in particular Gd, to river water as well (He et al., 2016; De Paula Marteleto and Enzweiler, 2021). This is indicated by appreciable positive Gd anomaly in wastewater (Fig. 5f), which has widely been reported to contain elevated concentration of anthropogenic Gd, in particular from drainage of hospital wastewater (Knappe et al., 1999; Bau and Dulski, 1996). Pearson correlation matrix suggested that REEs had a common origin (Fig. S9) and were mutually dependent on each other during transport. The good correlations between Gd and other REEs suggested that anthropogenic release not only affected Gd, but other REEs as well, likely because the

Gd and Nd used in MRI and industrial applications are not pure but contaminated by other REEs. High REE concentrations in rivers entering into Chaohu Lake were also attributed to agricultural and industrial production (Migaszewski and Galuszka, 2015; Jiang et al., 2022). Significant anthropogenic Gd anomalies were widely reported in the urban lakes (Liu et al., 2022c; Kreitsmann and Bau, 2023; Junqueira et al., 2024), reflecting anthropogenic impact of Gd on surface water.

Natural processes, such as chemical weathering and water-rock interactions, and infiltration of surface water usually control REE concentrations in groundwater. Groundwater showed normalized REE patterns like surface water with positive Gd anomaly, serving as an indicator of the anthropogenic impact. Rabiet et al. (2009) reported that $Gd/Gd^* > 1.4$ can be used to reflect anthropogenic Gd contamination in groundwater. Using this threshold, it can be found that 65% of groundwater samples were anthropogenically contaminated. Considering all surface water samples had Gd/Gd^* higher than 1.4, and that the highest Gd/Gd^* were observed in WWTP samples (Fig. 5), it is difficult to exclude the impact of wastewater and/or wastewater-contaminated surface water on groundwater. Stable isotope (D and ^{18}O) compositions indicated that groundwater and surface water samples located along LMWL (Fig. 3b), reflecting that both groundwater and surface water originated from precipitation. In this case, infiltration of mixture of rainwater and surface water was the plausible pathway by which anthropogenic REEs entered underground aquifer systems. Brünjes et al. (2016) suggested that anthropogenic Gd, which generated transient signals in surface water, could migrate into groundwater through riverbank infiltration. By using

anthropogenic Gd, infiltration of river water into shallow aquifers was quantitively assessed (Bichler et al., 2016). However, it is unclear, how long it should be taken for Gd to move from surface water to groundwater systems. Kulaksiz and Bau (2011) indicated that years to decades were needed for anthropogenic Gd-contaminated river water infiltrating into groundwater aquifers below Havel River, which made accumulation of anthropogenic Gd in tap water predictable over years. Accordingly, continuous field-based monitoring data combining modelling stimulation are needed to quantify Gd transport behavior.

4.2 Control on REE patterns

Groundwater was commonly enriched in HREEs relative to LREEs with negative Ce anomaly (Fig. 5). Enrichment of HREEs patterns was related to REE speciation in groundwater (Ma et al., 2023; Liu et al., 2024). This was due to (i) carbonate and sulfate complexes, and free ion were predicted to be the main REE solution species, whereby complexation of REEs with sulfate was unexpected to fractionate REE because of the relatively stable REE-sulfate formation constants (Schijf and Byrne, 2004; Wilkin et al., 2021; Liu et al., 2022b); (ii) association of REEs with carbonate preferentially stabilized HREEs, leading to an enrichment of HREEs over LREEs (Luo and Byrne, 2004; Guo et al., 2010); and (iii) REE adsorption onto mineral surfaces was unsignificant under the slightly acidic to circumneutral pH environments. The weak correlation between REE and Fe or Mn concentrations indicated that scavenging by Fe and Mn oxyhydroxides was limited (Fig. S9). Lozano et al. (2020) demonstrated that distribution coefficients of REEs between Fe oxyhydroxides and solution showed a

very weak increase with increasing atomic numbers at pH of 6.3 to 6.8, whereby adsorption by these minerals scarcely contributed to HREEs enrichment. Therefore, carbonate solute complexation was the main cause for HREEs-enriched patterns in groundwater, and free REE ions facilitated REE mobilization with groundwater flow.

Normalized REE patterns for surface water were relatively complex. This was attributed to the influence of both natural processes and anthropogenic activities. The enrichment of HREEs found in all of Fu River and Ganjiang River samples was mainly controlled by weathering of parent rocks and solutes complexation. Possible REEs-bearing minerals including bastnaesite-(Y), monazite, xenotime, and zircon were found to occur in the study area (Meng and Li, 2007), though more information on mineral compositions in aquifer sediments is necessary to clarify on this relationship. The humic climate in southern China favors weathering of minerals, especially bastnaesite-(Y), which highly enrich HREEs (Bao and Zhao, 2008). Hence, the fractionation degree between LREEs and HREEs was largely determined by mineral resistance to weathering. During weathering processes, the preferentially mobilized REEs are complexed by main anions in solutions, whereby HREEs exhibited greater affinities for CO_3^{2-} as compared to LREEs (Guo et al., 2010). Indeed, sums of proportion of REE-CO_3^{+} and REE-$(CO_3)_2^{-}$ were higher for surface water than groundwater, while proportion of REE^{3+} was lower in surface water (Fig. 6), leading to enrichments of HREEs in Fu River and Ganging River. Surface water samples from Rao River, Xin River, and Xiu River showed LREEs-enriched patterns as well, which may be due to anthropogenic impact. A previous study on Poyang Lake showed that

anthropogenic sources of REEs were enriched in LREEs (Wang et al., 2019). In fact, LREEs were widely used in petroleum refining as catalysts producing gasoline and fuel oil (Nieto et al., 2013; Alonso et al., 2023), and agricultural fertilizers contained LREEs-enriched phosphate minerals (i.e., galena and apatite) (Ribeiro et al., 2021). The spatial heterogeneity in REE patterns indicated their different sources and diverse cycling pathways (Junqueira et al., 2024). These results suggested that the REE compositions in surface water were influenced by release of REEs-enriched substances from natural processes and human activities.

4.3 Tracing the potential impact of anthropogenic Gd

4.3.1 Determination of anthropogenic Gd

Since anthropogenic input is found to be an important source of REEs to waters in the study area, it is essential to quantify the amount of REEs that were derived from anthropogenic activities. Gadolinium is the most widely reported anthropogenic REE due to extensive use of Gd-based contrast reagent in hospitals for medical diagnosis (Song et al., 2017; Thomsen, 2017; Inoue et al., 2020). Various Gd anomaly (Gd/Gd*) values including 1.1 (Lawrence, 2010), 1.15 (Lawrence et al., 2009), 1.2 (Bau et al., 2006), 1.3 (Petelet-Giraud et al., 2009), 1.4 (Rabiet et al., 2009), and 1.5 (Rozemeijer et al., 2012) were previously used as a threshold to differentiate anthropogenic Gd from natural occurring Gd (Rabiet et al., 2009). However, only Rabiet et al. (2009) was working with groundwater conditions. Therefore, Gd/Gd* of 1.4 was used as a threshold in this study to determine the anthropogenic Gd (Gd_{anth}) concentrations,

which equaled to the difference between measured Gd concentration (Gd_{mea}) and geogenic background concentration (Gd*). The latter was calculated by interpolation using normalized values of Sm and Tb Eqs. (7) and (8).

$$Gd_{anth} = Gd_{mea} - Gd^* \quad \text{Eq. (7)}$$

$$Gd^* = (Sm_{UCC}^{0.33} + Tb_{UCC}^{0.67}) \cdot 3.8 \quad \text{Eq. (8)}$$

The obtained results showed that Gd_{anth} concentrations ranged from 6.2 ng/L to 37.2 ng/L in surface water with 8.7 ng/L to 37.2 ng/L (average 16.1 ng/L) for Rao River, 10.5 ng/L to 17.5 ng/L (average 14.6 ng/L) for Xin River, 9.9 ng/L to 14.1 ng/L (average 12.3 ng/L) for Fu River, 10.6 ng/L to 20.2 ng/L (average 14.1 ng/L) for Ganjiang River, and 6.2 ng/L to 12.9 ng/L (average 9.9 ng/L) for Xiushui River. Gd_{anth} concentrations thus accounted for 73%, 71%, 68%, 61%, and 52% of the total Gd concentrations in Ganjiang River, Xiushui River, Rao River, Xin River, and Fu River, respectively. This indicated that Ganjiang River was most strongly contaminated by anthropogenic Gd among the five rivers. The Gd_{anth} concentrations were comparable to the values published in Peng (2020), showing Gd_{anth} concentrations ranged between 1.7 ng/L and 16.1 ng/L in Suzhou River, an inland urban river in southern China. A similar range of Gd_{anth} concentrations (1.6 ng/L to 12.6 ng/L) in Han River was reported by Kim et al. (2020).

Gd_{anth} concentrations ranged from 4.6 ng/L to 63.8 ng/L in groundwater. The largest Gd_{anth} concentrations were found in groundwater samples taken along the banks of Xin River (6.65 ng/L to 63.84 ng/L, average 28.24 ng/L), followed by those of Xiushui River (5.61 ng/L to 28.36 ng/L, average 15.72 ng/L), Fu River (9.69 ng/L to

19.67 ng/L, average 13.02 ng/L), Rao River (4.57 ng/L to 17.85 ng/L, average 12.32 ng/L), and Ganjiang River (5.61 ng/L to 17.16 ng/L, average 10.83 ng/L). It is interesting to note that Gd_{anth} concentrations in groundwater taken along the bank of Ganjiang River occupied up to 73% of total Gd concentrations in average, while average proportion of Gd_{anth} concentrations were 68%, 63%, 62%, and 61% in groundwaters of Fu River, Xinjiang River, Xiushui River, and Rao River, respectively. Therefore, Gd_{anth} concentrations in both groundwater and surface water confirmed a strong contamination status in Ganjiang River. The level of Gd_{anth} in the aquatic watersheds was closely related to population density and development of health systems (Kulaksiz and Bau, 2011; Schmidt et al., 2019; Brünjes and Hofmann, 2020). Barber et al. (2006) indicated that Gd_{anth} concentrations in watershed areas were connected to landscape (i.e., topography, ecology, geology, and land use) as well. Considering that >60% of the Poyang Lake area is covered by plains and hillocks (Liao et al., 2020; Mao et al., 2021), the heterogeneous distribution of Gd_{anth} concentrations largely reflected disparity in population and medical level in regions in the watersheds of the five rivers.

The quantification of anthropogenic REE contributions, particularly Gadolinium (Gd), underscores the significant impact of human activities on freshwater systems, necessitating comprehensive management strategies. The observed patterns of Gd contamination in both surface water and groundwater highlight the intricate relationship between anthropogenic inputs, regional development, and environmental health, emphasizing the need for localized interventions to mitigate pollution in watershed

areas.

4.3.2 Application of anthropogenic Gd to trace water contamination

To assess the feasibility of using Gd_{anth} to trace contamination in surface water and groundwater, the relationships between Gd_{anth} concentrations and some heavy metals concentrations were examined (Fig. 8). It's found that Gd_{anth} concentrations positively correlated with Pb, Co, Ni, as well as ΣREE concentrations in groundwater with correlation coefficients (R^2) as 0.72, 0.67, 0.45, and 0.99, respectively. The good relationships indicated that Gd_{anth} could serve as a good tracer of wastewater pollution in natural groundwater systems. This tracer effect was also observed in groundwater. The stability of Gd_{anth} compounds has resulted in a vast number of tracer studies in different hydrochemical environments (Möller et al., 2000; Klaver et al., 2014; Migaszewski and Gałuszka, 2015; De Paula Marteleto and Enzweiler, 2021; Liu et al., 2022c). Bichler et al. (2016) used Gd_{anth} to quantify river water infiltration into alluvial groundwater in western Europe, where Gd_{anth} was commonly detected in groundwater and bank filtrate due to wastewater discharges. Bank filtration of sewage-contaminated surface water was investigated using Gd_{anth} by Brünjes et al. (2016), showing that Gd_{anth} was an ideal indicator of sewage impact on both surface water and groundwater. The tracer effect of Gd_{anth} was suggested to generate a transient signal, which was due to working regulation of MRI facilities (i.e., weekdays) and patients' permanence in the hospital (Brünjes et al., 2016; De Paula Marteleto and Enzweiler, 2021). Combining with Sr and B isotopes, the Gd_{anth} was used to discriminate between natural and anthropogenic components influencing water quality in the Dommel Basin (Petelet-

Giraud et al., 2009). The traceability of Gd_{anth} in probing the impact of 9 trace elements concentrations on surface water was investigated by Peng (2020), who found a positive correlation between the proportions of Gd_{anth} and the trace element concentrations. It is worth noting that Gd_{anth} showed a linear relation with ΣREE and total Gd concentrations in surface water and groundwater (Fig. 8a). This demonstrated that Gd_{anth} could trace the anomalous accumulation of all REEs including Gd itself in aquatic systems, which have been considered as emerging contaminants due to their ever-increasing release into the environment (Ebrahimi and Barbieri, 2019; Lachaux et al., 2022). Consequently, anthropogenic discharge of REEs into freshwater environments comprises an opportunity for tracing other contaminants in aquatic systems.

Diverse regulatory approaches and management strategies for addressing anthropogenic Gd pollution reflect the regional disparities in REE contamination and environmental governance frameworks worldwide. While some regions have implemented stringent regulations to mitigate Gd pollution, others rely on monitoring programs and technological innovations to manage REE concentrations in freshwater ecosystems (Hashim et al., 2011).

4.4 Health risk evaluation

The anomalous appearance of REEs in groundwater, especially drinking water sources, because of anthropogenic activities has raised public concern (Knappe et al., 2005; Brünjes et al., 2016; Ebrahimi and Barbieri, 2019; Brouziotis et al., 2022). Both Gd and La were found to exhibit positive anomalies in surface water and groundwater, which has been widely attributed to anthropogenic activities (Kulaksiz and Bau, 2011;

2013; Klaver et al., 2014; Klein et al., 2022). Therefore, they were chosen as candidates to assess the non-carcinogenic risk by calculating their hazard quotient (HQ). Since groundwater is used for drinking water resources in the study area, human health risks are exposed to different population groups mainly through water ingestion exposure. The obtained HQ values of Gd (HQ_{Gd}) showed that it was $3.7\cdot10^{-5}$ to $1.3\cdot10^{-1}$ for infants, $2.3\cdot10^{-5}$ to $8\cdot10^{-2}$ for children, $1.6\cdot10^{-5}$ to $5.4\cdot10^{-2}$ for adult males, and $1.3\cdot10^{-5}$ to $4.5\cdot10^{-2}$ for adult females. For La, HQ_{La} values were $1.8\cdot10^{-3}$ to $4.6\cdot10^{-1}$ for infants, $1.1\cdot10^{-3}$ to $2.8\cdot10^{-1}$ for children, $7\cdot10^{-4}$ to $1.9\cdot10^{-1}$ for adult males, and $6\cdot10^{-4}$ to $1.6\cdot10^{-1}$ for adult females. Compared to groundwater, surface water had lower HQ values for both Gd and La (Fig. 9). All HQ values were <1, reflecting low carcinogenic risk of Gd and La in surface water and groundwater (USEPA, 2004). However, infants and children were subject to higher risk than adult males and females. Previous assessment results showed that HQ were $>1.8\cdot10^{-2}$ for children and $>3\cdot10^{-3}$ for adults (Guo et al., 2019; Sun et al., 2017), which were higher than average HQ ($9.9\cdot10^{-3}$) of children, while lower than average HQ of adults ($6.2\cdot10^{-3}$) observed in this study. Spatially, the distribution of HQ_{Gd} in groundwater indicated that people living in east of Poyang Lake suffered from higher health risk than those in the western part, especially around Rao River (Fig. 10). Among the five rivers, Rao River and Xin River generally had high HQ_{Gd}, while Ganjiang River and Xiushui River had low HQ_{Gd}, indicating that more serious carcinogenic risk was posed by Gd in groundwater taken from Rao River and Xin River, as compared to Ganjiang River and Xiushui River, which was the case for all population groups.

641 However, it should be noted that both infants and children were suggested to be
642 more sensitive to contamination than adults via ingestion pathway, owing to hand-
643 mouth activity, low body weight, and incomplete physiologic systems (Rodríguez-
644 Barranco et al., 2014), as indicated by higher HQ_{La} and HQ_{Gd} for infants and children.
645 Jin et al. (2014) performed REE health risk assessments in REE-contaminated areas of
646 Jiangxi province, showing that average daily intake of REEs through ingestion of crops
647 and groundwater was 295 μg/kg/d, which was four times higher than safe dosage (70
648 μg/kg/d) and near three times of subclinical threshold (100 to 110 μg/kg/d) (Zhu et al.,
649 1997; Li et al., 2013). Su et al. (1985) indicated that the average daily intake of REEs
650 was 1.75 mg and 2.25 mg for people living in south and north of China, respectively,
651 with 0.1 mg from drinking water, which was estimated based on REE exposure
652 pathways. These authors assessed REE health risks based on humans' lifetime average
653 daily intake dose of REEs without considering different crowds (Jin et al., 2014).
654 Fortunately, anthropogenic REEs contamination in groundwater has received public
655 concern (Knappe et al., 2005; Rabiet et al., 2009; Brünjes et al., 2016). Studies
656 concerning REE health risk are increasing also in developing countries where higher
657 REE health and ecological risks may occur (Gwenzi et al., 2018). The potential human
658 health impact induced by exposure to REEs was comprehensively reviewed by
659 Brouziotis et al. (2022), pointing out that the existing literature about REE toxicity to
660 human health was focused on their cytotoxicity to human cell lines, and matrices like
661 hair, blood, and blood serum were studied more extensively. Hopefully, the linkage
662 between REE dietary intake from drinking water and human health could be better

established in the future on basis of in-depth research on REE exposure route and biomonitoring.

The assessment of non-carcinogenic risks associated with anthropogenic REEs like Gd underscores the interdisciplinary approach required, integrating insights from environmental science, toxicology, public health, and policy studies (Libralato et al., 2023), especially considering that REEs are now regarded as emerging pollutants (Trapasso, 2020; Falandysz et al., 2024). Recent studies have highlighted the heightened vulnerability of infants and children to contamination (Wang et al., 2022), reflecting the importance of interdisciplinary research in understanding and mitigating the health impacts of REE pollution. Hopefully, more further investigations to reinforce a cause-effect relationship between pathological status and REE exposure will emerge in recent future.

5. Conclusions

Surface water, wastewater, and groundwater samples were collected from Poyang Lake basin to investigate REE geochemical behavior and the impact of anthropogenic activities. Results showed that groundwater was weakly acidic to neutral with pH 4.5 to 7.5, and surface water with higher pH of 6.53 to 9.23. Total REE (ΣREE) concentrations ranged from 0.5 μg/L to 416 μg/L, and from 0.40 μg/L to 1.33 μg/L with average 10.1 μg/L and 0.80 μg/L in groundwater and surface water, respectively. Wastewater had higher total REE concentrations (231 to 904μg/L), much higher than both surface water and groundwater. High-REEs water samples were of Ca-Mg-Cl/SO_4

hydrochemical type, and tended to deviate from local meteoric water line in $\delta^{18}O$-δD plot. REE species was dominated by free ion, carbonate and sulfate complexes in both surface water and groundwater. All water samples were characterized by positive Gd anomaly, and positive Gd anomaly was observed in both influent and effluent samples of wastewater treatment plants, which reflected anthropogenic impact by Gd on both surface water and groundwater. Anthropogenic Gd was making up 4% to 21%, and 49% to 84% of total Gd concentrations in surface water and groundwater, respectively. The relatively complex normalized REE pattern in surface water was related to both anthropogenic input and natural processes such as chemical weathering and solution complexation. The HREEs-enriched patterns of groundwater were formed mainly through carbonate solution complexation. Anthropogenic Gd could act as a tracer not only of REEs, but also trace metal pollution in groundwater, because positive correlations were found between anthropogenic Gd concentrations and REE, Pb, Ni, and Co concentrations. Based on human health risk evaluation results, it was found that groundwater had higher hazard quotient (HQ) with regard to Gd than surface water, and infants and children suffered from higher risk than adult males and females. A similar spatial distribution of HQ_{Gd} in groundwater was observed for the four population groups, showing higher values in the east of Poyang Lake than in the western part. Overall, our findings highlight the significant influence of anthropogenic activities on the geochemical behavior of REE in the Poyang Lake basin, underscoring the importance of continued monitoring and management efforts to mitigate potential environmental risks associated with metal pollution.

707

Acknowledgement

The study was financially supported by the National Natural Science Foundation of China (Nos. 42262029 and 41825017), Natural Science Foundation of Jiangxi Province, China (Nos. 20232BAB203066 and 20202BABL211018), East China University of Technology Research Foundation for Advanced Talents (Nos. DHBK2019094 and SHT201901), and Jiangxi Provincial Key Laboratory of Genesis and Remediation of Groundwater Pollution (No. 2023SSY02041). We thank the anonymous reviewers, Michael Kersten, and Associate Editor Dan Lapworth for their helpful suggestions and comments.

References

Adeel, M., Lee, J.Y., Zain, M., Rizwan, M., Nawab, A., Ahmad, M., Shafiq, M., Yi, H., Jilani, G., Javed, R., 2019. Cryptic footprints of rare earth elements on natural resources and living organisms. Environ. Int. 127, 785-800.

Alonso, E., Pineault, D.G., Gambogi, J., Nassar, N.T., 2023. Mapping first to final uses for rare earth elements, globally and in the United States. J. Ind. Ecol. 27(1), 312-322.

Aubert, D., Stille, P., Probst, A., 2001. REE fractionation during granite weathering and removal by waters and suspended loads: Sr and Nd isotopic evidence. Geochim. Cosmochim. Acta 65(3), 387-406.

Bao, Z., Zhao, Z., 2008. Geochemistry of mineralization with exchangeable REY in the weathering crusts of granitic rocks in South China. Ore Geol. Rev. 33(3-4), 519-

535.

Barber, L.B., Murphy, S.F., Verplanck, P.L., Sandstrom, M.W., Taylor, H.E., Furlong, E.T., 2006. Chemical loading into surface water along a hydrological, biogeochemical, and land use gradient-a holistic watershed approach. Environ. Sci. Technol. 40, 475-486.

Barroux, G., Sonke, J.E., Boaventura, G., Viers, J., Godderis, Y., Bonnet, M. P., Sondag, F., Gardoll, S., Lagane, C., Seyler, P., 2006. Seasonal dissolved rare earth element dynamics of the Amazon River main stem, its tributaries, and the Curuaí floodplain. Geochem. Geophy. Geosy. 7(12).

Bau, M., Dulski, P., 1996. Anthropogenic origin of positive gadolinium anomalies in river waters. Earth Planet Sci. Lett. 143, 245-55.

Bau, M., Knappe, A., Dulski, P., 2006. Anthropogenic gadolinium as a micropollutant in river waters in Pennsylvania and in Lake Erie, northeastern United States. Chem. Erde 66, 143-152.

Bernstein, E.J., Schmidt-Lauber, C., Kay, J., 2012. Nephrogenic systemic fibrosis: a systemic fibrosing disease resulting from gadolinium exposure. Best Pract. Res. Clin. Rheumatol. 26(4), 489-503.

Bichler, A., Muellegger, C., Brünjes, R., Hofmann, T., 2016. Quantification of river water infiltration in shallow aquifers using acesulfame and anthropogenic gadolinium. Hydrol. Process. 30(11), 1742-1756.

Brouziotis, A.A., Giarra, A., Libralato, G., Pagano, G., Guida, M., Trifuoggi, M., 2022. Toxicity of rare earth elements: An overview on human health impact. Front.

Env. Sci. 10, 948041.

Brünjes, R., Hofmann, T., 2020. Anthropogenic gadolinium in freshwater and drinking water systems. Water Res. 182, 115966.

Brünjes, R., Bichler, A., Hoehn, P., Lange, F.T., Brauch, H.J., Hofmann, T., 2016. Anthropogenic gadolinium as a transient tracer for investigating river bank filtration. Sci. Total Environ. 571, 1432-1440.

Caravan, P., Ellison, J.J., McMurry, T.J. Lauffer, R.B., 1999. Gadolinium(III) chelates as MRI contrast agents: Structure, dynamics, and applications. Chem. Rev. 99, 2293-2352.

Cassee, F.R., van Balen, E.C., Singh, C., Green, D., Muijser, H., Weinstein, J., Dreher, K., 2011. Exposure, health and ecological effects review of engineered nanoscale cerium and cerium oxide associated with its use as a fuel additive. Crit. Rev. Toxicol. 41,213-229.

Chen, M., Zeng, S., Jiang, B., Wen, Z., Wu, J., Xia, J., 2023. The comprehensive evaluation of how water level fluctuation and temperature change affect vegetation cover variations at a lake of ecological importance (Poyang Lake), China. Ecol. Indic. 148, 110041.

Chen, Z., Zhu, X., 2008. Accumulation of rare earth elements in bone and its toxicity and potential hazard to health. Rural Eco. Environ. 24, 256-257.

Chu, X.D., 2022. Regional groundwater environment evolution and partition the prevention-control in urban agglomeration around Poyang Lake. PhD dissertation. Nanchang University. Jiangxi Province. China.

De Paula Marteleto, T., Enzweiler, J., 2021. Anthropogenic gadolinium as a tracer of raw sewage in surface water. Environ. Earth Sci. 80(17), 607.

Doronin, V., Sorokina, T., Lipin, P., Potapenko, O., Korotkova, N., Gordenko, V., 2015. Development and introduction of zeolite containing catalysts for cracking with controlled contents of rare earth elements. Catal. Index 7 (1), 12-16.

Ebrahimi, P., Barbieri, M., 2019. Gadolinium as an emerging microcontaminant in water resources: Threats and opportunities. Geosciences 9, 93.

Falandysz, J., Liu, G., Rutkowska, M., 2024. Analytical Progress on Emerging Pollutants in the Environment: An Overview of the Topics. Trac Trends Anal. Chem. 117719.

Feng, L., Hu, C., Chen, X., Zhao, X., 2013. Dramatic inundation changes of China's two largest freshwater lakes linked to the Three Gorges Dam. Environ. Sci. Technol. 47 (17), 9628-9634.

Gaillardet, J., Viers, J., Dupré, B., 2005. Trace elements in river waters. In Surface and Ground Water, Weathering, and Soils. Treatises on Geochemistry, Vol. 5 (ed. J. I. Drever). Elsevier, Amsterdam, pp. 225-272.

Goldstein, S.J., Jacobsen, S.B., 1988. Rare earth elements in river waters. Earth Planet. Sci. Lett. 89(1), 35-47.

Golroudbary, S.R., Makarava, I., Kraslawski, A., Repo, E., 2022. Global environmental cost of using rare earth elements in green energy technologies. Sci. Total Environ. 832, 155022.

González, V., Vignati, D.A.L., Pons, M.N., Montarges-Pelletier, E., Bojic, C.,

Giamberini, L., 2015. Lanthanide ecotoxicity: first attempt to measure environmental risk for aquatic organisms. Environ. Pollut. 199, 139-147.

Guo, G.H., Song, B., Lei, M., Wang, Y.W., 2019. Rare earth elements (REEs) in PM10 and associated health risk from the polymetallic mining region of Nandan County, China. Hum. Ecol. Risk Assess. 25(3), 672-687.

Guo, H.M., Zhang, B., Wang, G.C., Shen, Z.L., 2010. Geochemical controls on arsenic and rare earth elements approximately along a groundwater flow path in the shallow aquifer of the Hetao Basin, Inner Mongolia. Chem. Geol. 270, 117-125.

Gwenzi, W., Mangori, L., Danha, C., Chaukura, N., Dunjana, N., Sanganyado, E., 2018. Sources, behaviour, and environmental and human health risks of high-technology rare earth elements as emerging contaminants. Sci. Total. Environ. 636, 299-313.

Han, G.L., Liu, C.Q., 2007. Dissolved rare earth elements in river waters draining karst terrains in Guizhou Province, China. Aquat. Geochem. 13, 95-107.

Hashim, M.A., Mukhopadhyay, S., Sahu, J.N., Sengupta, B., 2011. Remediation technologies for heavy metal contaminated groundwater. J. Environ. Manag. 92, 2355-2388.

Haskin, M.A., Haskin, L.A., 1966. Rare earths in European shales: a redetermination. Science 154, 507-509.

Hatje, V.; Bruland, K.W.; Flegal, A.R., 2016. Increases in anthropogenic gadolinium anomalies and rare earth rlement concentrations in San Francisco Bay over a 20 year record. Environ. Sci. Technol. 50, 4159-4168.

He, J., M, N., Kuang, Y.C., Fan, Q.Y., Wang, X., Guan, W., Li, G.M., Li, C.S., Wang,

X.W., 2005. Speciation and distribution characters of rare earth elements in the Baotou section of the Yellow river. Environ. Sci. 25(2), 61-66. (in Chinese with English abstract).

He, W., Bai, Z.L., Liu, W.X., Kong, X.Z., Yang, B., Yang, C., Jorgensen, S.E., Xu, F.L., 2016. Occurrence, spatial distribution, sources, and risks of polychlorinated biphenyls and heavy metals in surface sediments from a large eutrophic Chinese lake (Lake Chaohu). Environ. Sci. Pollut. Res. 23 (11), 10335-10348.

Hu, Z., Haneklaus, S., Sparovek, G., Schnug, E., 2006. Rare earth elements in soils. Commun. Soil Sci. Plan 37, 1381-1420.

Hummel,W., Berner, U., Curti, E., Pearson, F.J., Thoenen, T., 2002. Nagra/PSI chemical thermodynamic Data Base 01/01. Radiochim. Acta 90, 805-813.

Inoue, K., Fukushi, M., Furukawa, A., Sahoo, S. K., Veerasamy, N., Ichimura, K., Kasahara, S., Ichihara, M., Tsukada, M., Torii, M., Mizoguchi, M., Taguchi, Y., Nakazawa, S., 2020. Impact on gadolinium anomaly in river waters in Tokyo related to the increased number of MRI devices in use. Mar. Pollut. Bull. 154, 111148.

Jiang, C.L., Li, Y.H., Li, C., Zheng, L.L., Zheng, L.G., 2022. Distribution, source and behavior of rare earth elements in surface water and sediments in a subtropical freshwater lake influenced by human activities. Environ. Pollut. 313, 120153.

Jin, S.L, Huang, Y.Z., Hu, Y., Qiao, M., Wang, X.L., Wang, F., Li, J., Xiang, M., Xu, F., 2014. Rare earth elements content and health risk assessment of soil and crops in typical rare earth mine area in Jiangxi province. Acta Sci. Circum. 34(12), 3084-

3093. (in Chinese with English abstract)

Jin, G.E., Hong, X.Y., Wang, X.X., Yao, W.S., Zhang, J.Y., Gong, Z.B., 2010. Geochemical characteristics of rare earth elements in Jiulongjiang estuary. J. Oceanogr. Taiwan Strait 29(3), 304-313. (in Chinese with English abstract)

Johannesson, K.H., Palmore, C.D., Fackrell, J., Prouty, N.G., Swarzenski, P.W., Chevis, D.A., Telfeyan, K., White, C.D., Burdige, D.J., 2017. Rare earth element behavior during groundwater-seawater mixing along the Kona Coast of Hawaii. Geochim. Cosmochim. Acta 198, 229-258.

Junqueira, T., Beckner-Stetson, N., Richardson, V., Leybourne, M. I., Vriens, B., 2024. Rare earth element distribution patterns in Lakes Huron, Erie, and Ontario. J. Hydrol. 629, 130652.

Kim, I., Kim, S. H., Kim, G., 2020. Anthropogenic gadolinium in lakes and rivers near metrocities in Korea. Environ. Sci-Proc. Imp. 22(1), 144-151.

Klaver, G., Verheul, M., Bakker, I., Petelet-Giraud, E., Négrel, P., 2014. Anthropogenic rare earth element in rivers: gadolinium and lanthanum. Partitioning between the dissolved and particulate phases in the Rhine River and spatial propagation through the Rhine-Meuse Delta (the Netherlands). Appl. Geochem. 47, 186-197.

Klein, O., Zimmermann, T., Hildebrandt, L., Pröfrock, D., 2022. Technology-critical elements in Rhine sediments-A case study on occurrence and spatial distribution. Sci. Total Environ. 852, 158464.

Knappe, A., Möller, P., Dulski, P., Pekdeger, A., 2005. Positive gadolinium anomaly in surface water and ground water of the urban area Berlin, Germany. Geochem.

65(2), 167-189.

Knappe, A., Sommer-von Jarmersted, C., Pekdeger, A., Bau, M., Dulski, P., 1999. Gadolinium in aquatic systems as indicator for sewage water contamination. In: Armannsson, H. (Ed.), Proceedings of the Fifth International Symposium on Geochemistry of the Earth's Surface, Reykjavic, 16-20 August, A.A. Balkema Publishers, Rotterdam, pp. 187-190.

Kreitsmann, T., Bau, M., 2023. Rare earth elements in alkaline Lake Neusiedl, Austria, and the use of gadolinium microcontamination as water source tracer. Appl. Geochem. 159, 105792.

Kulaksiz, S., Bau, M., 2013. Anthropogenic dissolved and colloid/nanoparticle bound samarium, lanthanum and gadolinium in the Rhine River and the impending destruction of the natural rare earth element distribution in rivers. Earth Planet Sci. Lett. 362, 43-50.

Kulaksiz, S., Bau, M., 2011. Rare earth elements in the Rhine river, Germany: first case of anthropogenic lanthanum as a dissolved microcontaminant in the hydrosphere. Environ. Int. 37(5), 973-979.

Lachaux, N., Cossu-Leguille, C., Poirier, L., Gross, E.M., Giamberini, L., 2022. Integrated environmental risk assessment of rare earth elements mixture on aquatic ecosystems. Front. Environ. Sci. 10, 974191.

Lawrence, M.G., 2010. Detection of anthropogenic gadolinium in the brisbane river plume in moreton bay, Queensland, Australia. Mar. Pollut. Bull. 60, 1113-1116.

Lawrence, M.G., Ort, C., Keller, J., 2009. Detection of anthropogenic gadolinium in

884 treated wastewater in South East Queensland, Australia. Water Res. 43, 3534-3540.
885 Li, X.F., Chen, Z.B., Chen, Z.Q., Zhang, Y.H., 2013. A human health risk assessment
886 of rare earth elements in soil and vegetables from a mining area in Fujian Province,
887 Southeast China. Chemosphere 93(6), 1240-1246.
888 Li, Y.C., Gong, Z.B., Li, J., Wen, Y.Y., Wang, T., 2005. Inductively coupled plasma-
889 mass spectrometric determination of rare earth elements in estuarine water with
890 co-precipitation pre-concentration. J. Instrum. Anal. 24(1), 12-16. (In Chinese
891 with English abstract)
892 Liao, F., Wang, G.C., Yi, L.X., Shi, Z.M., Cheng, G.Q., Kong, Q.M., Mu, W.Q., Guo,
893 L., Cheng, K., Dong, N., Liu, C.L., 2020. Identifying locations and sources of
894 groundwater discharge into Poyang Lake (eastern China) using radium and stable
895 isotopes (deuterium and oxygen-18). Sci. Total Environ. 740, 140163.
896 Libralato, G., Davranche, M., Vantelon, D., Bau, M., Johannesson, K. H., 2023. Further
897 rare earth elements environmental dissemination: Observation, analysis, and
898 impacts. Front. Earth Sci. 11, 1182827.
899 Liu, X.R., Liu, W.S., Zhang, M., Jin, C., Ding, K.B., Baker, A.J., Liu, R.L., Tang, Y.T.,
900 Wang, S.Z., 2024. Organic-mineral colloids regulate the migration and
901 fractionation of rare earth elements in groundwater systems impacted by ion-
902 adsorption deposits mining in South China. Water Research, 256, 121582.
903 Liu, Z., Gu, X., Lian, M., Wang, J., Xin, M., Wang, B., Ouyang, W., He, M., Liu, X.,
904 Lin, C., 2023. Occurrence, geochemical characteristics, enrichment, and
905 ecological risks of rare earth elements in sediments of “the Yellow river-Estuary-

bay" system. Environ. Pollut. 319, 121025.

Liu, H.Y., Guo, H.M., Pourret, O., Wang, Z., Liu, M.H., Zhang, W.M., Li, Z.B., Gao, B., Sun, Z.X., Laine, P., 2022a. Geochemical signatures of rare earth elements and yttrium exploited by acid solution mining around an ion-adsorption type deposit: role of source control and potential for recovery. Sci. Total Environ. 804, 150241.

Liu, M.H., Liu, H.Y., Zhang, W.M., Wang, Z., Wu, T.H., Wang, Y.G., 2022b. REE concentration and fractionation in waters and sediments from the northern branch of Ganjiang River, Poyang Lake catchment. Geoscience 36(2), 389-405. (In Chinese with English abstract).

Liu, Y., Wu, Q., Jia, H., Wang, Z., Gao, S., Zeng, J., 2022c. Anthropogenic rare earth elements in urban lakes: Their spatial distributions and tracing application. Chemosphere, 300, 134534.

Liu, H.Y., Guo, H.M., Xing, L.N., Zhan, Y.H., Li, F.L., Shao, J.L., N, H., L, X., Li, C.Q., 2016. Geochemical behaviors of rare earth elements in groundwater along a flow path in the North China Plain. J. Asian Earth Sci. 117, 33-51.

Lozano, A., Ayora, C., Macías, F., Léon, R., Gimeno, M.J., Auqué, L., 2020. Geochemical behavior of rare earth elements in acid drainages: modeling achievements and limitations. J. Geochem. Explor. 216, 106577.

Luo, Y.R., Byrne, R.H., 2004. Carbonate complexation of yttrium and the rare earth elements in natural waters. Geochim. Cosmochim. Acta 68, 691-699.

Ma, S., Han, G., Yang, Y., Li, X., 2023. Geochemistry of dissolved rare earth elements in the Lancang River with cascade dams and implications for anthropogenic

impacts. Appl. Geochem. 159, 105854.

Ma, L., Wang, W.X., 2023. Dissolved rare earth elements in the Pearl River Delta: Using Gd as a tracer of anthropogenic activity from river towards the sea. Sci. Total Environ. 856, 159241.

Mao, H., Wang, G., Rao, Z., Liao, F., Shi, Z., Huang, X., Yang, Y., 2021. Deciphering spatial pattern of groundwater chemistry and nitrogen pollution in Poyang Lake Basin (eastern China) using self-organizing map and multivariate statistics. J. Clean. Prod. 329, 129697.

Meng, X.L., 2007. Geochemical characteristics of dissolved rare earth elements in water bodies of small watershed in southern Jiangxi Province. Chin. Rare Earth. 5, 625-631.

Meng, X.L., Ji, H.B., 2007. Contents and distribution pattern of dissolved rare earth elements in Ganjiang River in the southern Jiangxi province. J. Chin. Rare Earth Soc. 25(5), 625-631.

Mesa, F., Magán-Fernández, A., Muñoz, R., Papay-Ramírez, L., Poyatos, R., Sánchez-Fernández, E., Galindo-Moreno, P., Rodríguez-Barranco, M., 2014. Catecholamine metabolites in urine, as chronic stress biomarkers, are associated with higher risk of chronic periodontitis in adults. J. periodontal. 85(12), 1755-1762.

Migaszewski, Z.M., Gałuszka, A., 2015. The characteristics, occurrence and geochemical behavior of rare earth elements in the environment: a review. Crit. Rev. Environ. Sci. Technol. 45, 429-471.

Möller, P., Dulski, P., Bau, M., Knappe, A., Pekdeger, A., Sommer-von Jarmersted, C., 2000. Anthropogenic gadolinium as a conservative tracer in hydrology. J. Geochem. Explor. 69, 409-414.

Möller, P., Paces, T., Dulski, P., Morteani, G., 2002. Anthropogenic Gd in surface water, drainage system, and the water supply of the City of Prague, Czech Republic. Environ. Sci. Technol. 36, 2387-2394.

Munemoto, T., Ohmori, K., Iwatsuki, T., 2015. Rare earth elements (REE) in deep groundwater from granite and fracture-filling calcite in the Tono area, central Japan: Prediction of REE fractionation in paleo- to present-day groundwater. Chem. Geol. 417, 58-67.

Nesbitt, H.W., 1979. Mobility and fractionation of rare earth elements during weathering of a granodiorite. Nature 279, 206-210.

Nieto, A., Guelly, K., Kleit, A., 2013. Addressing criticality for rare earth elements in petroleum refining: the key supply factors approach. Res. Pol. 38 (4), 496-503.

Noack, C.W., Dzombak, D.A., Karamalidis, A.K., 2014. Rare earth element distributions and trends in natural waters with a focus on groundwater. Environ. Sci. Technol. 48, 4317-4326.

Nozaki, Y., Lerche, D., Alibo, D.S., Tsutsumi, M., 2000. Dissolved indium and rare earth elements in three Japanese rivers and Tokyo Bay: evidence for anthropogenic Gd and In. Geochim. Cosmochim. Acta 64, 3975-82.

Pagano, G., Aliberti, F., Guida, M., Oral, R., Siciliano, A., Trifuoggi, M., Tommasi, F. 2015a. Rare earth elements in human and animal health: state of art and research

priorities. Environ. Res. 142, 215-220.

Pagano, G., Guida, M., Tommasi, F., Oral, R., 2015b. Health effects and toxicity mechanisms of rare earth elements-knowledge gaps and research prospects. Ecotoxicol. Environ. Saf. 115, 40-48.

Pagano, G., Tommasi, F., Guida, M., 2012. Comparative toxicity of cerium and of other rare earth elements (REEs) in plant and invertebrate test systems. Cerium: Molecular Structure, Technological Applications and Health Effects. Nova Science Publishers, Hauppauge, NY, USA, 107-124.

Parkhurst, D.L., Appelo, C.A.J., 2013. Description of input and examples for PHREEQC version 3-a computer program for speciation, batch-reaction, one-dimensional transport, and inverse geochemical calculations. US Geological Survey Techniques and Methods. 6, p. 497.

Pang, X., Li, D., Peng, A., 2002. Application of rare-earth elements in the agriculture of China and its environmental behavior in soil. Environ. Sci. Pollut. Res. 9, 143-148.

Peng, C.C., 2020. The composition characteristics and source analysis of dissolved rare earth elements and trace elements in surface water of Suzhou. Master dissertation. Guiyang university, Guiyang, China. (in Chinese).

Petelet-Giraud, E., Klaver, G., Negrel, P., 2009. Natural versus anthropogenic sources in the surface- and groundwater dissolved load of the Dommel river (Meuse basin): constraints by boron and strontium isotopes and gadolinium anomaly. J. Hydrol. 369, 336-349.

994 Port, M., Idee, J.M., Medina, C., Robic, C., Sabatou, M. and Corot, C., 2008. Efficiency,
995 thermodynamic and kinetic stability of marketed gadolinium chelates and their
996 possible clinical consequences: a critical review. Biometals 21, 469-490.
997 Pourret, O., Gruau, G., Dia, A., Davranche, M., Molénat, J., 2010. Colloidal control on
998 the distribution of rare earth elements in shallow groundwaters. Aquat. Geochem.
999 16(1), 31-59.
1000 Qin, J.F., Chen, X.Y., Li, Z.X., 2002. Effects of rare earth on human health. Guangdong
1001 Trace Elem. Sci. 9(6), 17. (in Chinese with English abstract).
1002 Rabiet, M., Brissaud, F., Seidel, J.L., Pistre, S., Elbaz-Poulichet, F., 2009. Positive
1003 gadolinium anomalies in wastewater treatment plant effluents and aquatic
1004 environment in the Hérault watershed (South France). Chemosphere 75, 1057-
1005 1064.
1006 Ramalho, M., Ramalho, J., Burke, L.M. Semelka, R.C., 2017. Gadolinium retention
1007 and toxicity-An update. Adv. Chronic Kidney D. 24, 138-146.
1008 Ribeiro, P.G., Dinali, G.S., Boldrin, P.F., de Carvalho, T.S., de Oliveira, C., Ramos,
1009 S.J., Siqueira, J.O., Moreira, C.G., Guilherme, L.R.G., 2021. Rare earth elements
1010 (REEs) rich-phosphate fertilizers used in Brazil are more effective in increasing
1011 legume crops yield than their REEs-poor counterparts. Int. J. Plant Prod. 15, 1-11.
1012 Rodushkin, I., Paulukat, C., Pontér, S., Engström, E., Baxter, D.C., Sörlin, D.,
1013 Pallavicini, N., Rodushkina, K., 2018. Application of double-focusing sector field
1014 icp-ms for determination of ultratrace constituents in samples characterized by
1015 complex composition of the matrix. Sci. Total Environ. 622-623, 203-213.

1016 Rozemeijer, J., Siderius, C., Verheul, M., Pomarius, H., 2012. Tracing the spatial
1017 propagation of river inlet water into an agricultural polder area using
1018 anthropogenic gadolinium. Hydrol. Earth Syst. Sci. 16, 2405-2415.
1019 Rue, G.P., McKnight, D.M., 2021. Enhanced rare earth element mobilization in a
1020 mountain watershed of the Colorado Mineral Belt with concomitant detection in
1021 aquatic biota: increasing climate change-driven degradation to water quality.
1022 Environ. Sci. Technol. 55(21), 14378-14388.
1023 Schijf, J., Byrne, R.H., 2004. Determination of SO_4ß1 for yttrium and the rare earth
1024 elements at I = 0.66 m and T = 25 °C - implications for YREE solution speciation
1025 in sulfate-rich waters. Geochim. Cosmochim. Acta 68, 2825-2837.
1026 Schmidt, K., Bau, M., Merschel, G., Tepe, N., 2019. Anthropogenic gadolinium in tap
1027 water and in tap water-based beverages from fast-food franchises in six major
1028 cities in Germany. Sci. Total Environ. 687, 1401-1408.
1029 Shin, S.H., Kim, H.Y., Rim, K.Y., 2019. Worker safety in the rare earth elements
1030 recycling process from the review of toxicity and issues. Saf. Health Work 10,
1031 409-419.
1032 Sholkovitz, E.R., 1993. The geochemistry of rare earth elements in the Amazon River
1033 Estuary. Geochim. Cosmochim. Acta 57, 2181-2190.
1034 Shvartsev, S., Shen, Z., Sun, Z., Wang, G., Soldatova, E., Guseva, N., 2016. Evolution
1035 of the groundwater chemical composition in the Poyang Lake catchment, China.
1036 Environ. Earth Sci. 75 (18), 1-16.
1037 Smedley, P.L., 1991. The geochemistry of rare earth elements in groundwater from the

Carnmenellis area, southwest England. Geochim. Cosmochim. Acta 55, 2767-2779.

Song, H., Shin, W.J., Ryu, J.S., Shin, H.S., Chung, H., Lee, K.S., 2017. Anthropogenic rare earth elements and their spatial distributions in the Han River, South Korea. Chemosphere 172, 155-165.

Squadrone, S., Brizio, P., Stella, C., Mantia, M., Battuello, M., Nurra, N., Abete, M.C., 2019. Rare earth elements in marine and terrestrial matrices of Northwestern Italy: Implications for food safety and human health. Sci. Total Environ. 660, 1383-1391.

Su, D.Z., Wang, J.Q., Wang, H.Z., 1985. Study on the content of rare earth element in plant food. J. Chin. Soci. of Rare Earth. Special Issue, 95-98. (in Chinese with English Abstract)

Sun, G.Y., Li, Z.G., Liu, T., Chen, J., Wu, T.T., Feng, X.B., 2017. Rare earth elements in street dust and associated health risk in a municipal industrial base of central China. Environ. Geochem. Hlth, 39(6), 1-18.

Takahashi, K., Nakamura, H., Furumoto, S., Yamamoto, K., Fukuda, H., Matsumura, A., Yamamoto, Y., Synthesis and in vivo biodistribution of BPA-Gd-DTPA complex as a potential MRI contrast carrier for neutron capture therapy, Bioorg. Med. Chem., 2005, 13(3), 735-743.

Tang, Y., Zhao, X., Jiao, J., 2020. Ecological security assessment of Chaohu Lake basin of China in the context of river chief system reform. Environ. Sci. Pollut. Res. 27 (3), 2773-2785.

Thomsen, H.S., 2006. Nephrogenic systemic fibrosis: a serious late adverse reaction to

gadodiamide. Eur. Radiol. 16(12), 2619-2621.

Thomsen, H.S., 2017. Are the increasing amounts of gadolinium in surface and tap water dangerous? Acta Radiol. 58, 259-263.

Trapasso, G., 2020. Gadolinium as an emerging pollutant: a review on its occurrence and impacts in aquatic ecosystems. Available online at: http://dspace.unive.it/handle/10579/17685.

USEPA., 2004. USEPA claims to meet drinking water goals despite persistent data quality shortcomings. Report no. 2004-P-0008. Available online at www.epa.gov/ oig/reports/2004/20040305-2004-P-0008.pdf.

USEPA, 1989. Risk Assessment Guidance for Superfund, Volume I: Human Health Evaluation Manual (Part A), Interim Final. Washington, DC.

Verplanck, P.L. 2013. Partitioning of rare earth elements between dissolved and colloidal phases. Proced. Earth Planet. Sci. 7, 867-870.

Vergauwen, E., Vanbinst, A.M., Brussaard, C., Janssens, P., De Clerck, D., Van Lint, M., Houtman, A.C., Michel, O., Keymolen, K., Lefevere, B., Bohler, S., 2018. Central nervous system gadolinium accumulation in patients undergoing periodical contrast MRI screening for hereditary tumor syndromes. Hereditary Cancer Clin. Pract. 16(1), 2.

Wang, L., Han, X., Liang, T., Guo, Q., Li, J., Dai, L., Ding, S., 2019. Discrimination of rare earth element geochemistry and co-occurrence in sediment from Poyang Lake, the largest freshwater lake in China. Chemosphere 217, 851-857.

Wang, W., Yang, P., Xia, J., Huang, H., Li, J., 2023. Impact of land use on water quality

in buffer zones at different scales in the Poyang Lake, middle reaches of the Yangtze River basin. Sci. Total Environ. 896, 165161.

Wang, Y., Wang, G., Sun, M., Liang, X., He, H., Zhu, J., Takahashi, Y., 2022. Environmental risk assessment of the potential “Chemical Time Bomb” of ion-adsorption type rare earth elements in urban areas. Sci. Total Environ. 822, 153305.

Wang, T., Wu, Q.X., Wang, Z.H., Dai, G., Jia, H.P., Gao, S.L., 2021. Anthropogenic gadolinium accumulation and rare earth element anomalies of river water from the middle reach of Yangtze River Basin, China. ACS Earth Space Chem. 5(11), 3130-3139.

Wilkin, R.T., Lee, T.R., Ludwig, R.D., Wadler, C., Brandon, W., Mueller, B., Davis, E., Luce, D., Edwards, T., 2021. Rare-earth elements as natural tracers for in situ remediation of groundwater. Environ. Sci. Technol. 55 (2), 1251-1259.

Xiao, Y., Hao, Q., Zhang, Y., Zhu, Y., Yin, S., Qin, L., Li, X., 2022. Investigating sources, driving forces and potential health risks of nitrate and fluoride in groundwater of a typical alluvial fan plain. Sci. Total Environ. 802, 149909.

Xie, X.J., Wang, Y.X., Li, J.X., Su, C.L., Wu, Y., Yu, Q., Li, N.D., 2012. Characteristics and implications of rare earth elements in high arsenic groundwater from the Datong basin. Earth Sci. 37(2), 381-390. (in Chinese with English Abstract)

Xu, Z.F., Han, G.L., 2009. Rare earth elements (REE) of dissolved and suspended loads in the Xijiang River, South China. Appl. Geochem. 24(9), 1803-1816.

Zhan, L., Chen, J., Zhang, S., Li, L., Huang, D., Wang, T., 2016. Isotopic signatures of

precipitation, surface water, and groundwater interactions, Poyang Lake Basin, China. Environ. Earth Sci. 75, 1307.

Zhang, J., Wang, Z., Wu, Q., An, Y., Jia, H., Shen, Y., 2019. Anthropogenic rare earth elements: Gadolinium in a small catchment in Guizhou Province, Southwest China. Int. J. Env. Res. and Pub He. 16(20), 4052.

Zhang, H., Jiang, Y.H., Wang, M., Wang, P., Shi, G.X., Ding, M.J., 2017. Spatial characterization, risk assessment, and statistical source identification of the dissolved trace elements in the Ganjiang River-feeding tributary of the Poyang Lake, China. Environ. Sci. Pollut. R. 24 (3), 2890-2903.

Zhang, L.Y., 1986. Research report of the quaternary geology for the Poyang Lake region in Jiangxi province. National Geological Information Data Center.

Zheng, L., Wang, X., Li, D., Xu, G., Guo, Y., 2021. Spatial heterogeneity of vegetation extent and the response to water level fluctuations and micro-topography in Poyang Lake, China. Ecol. Indic. 124, 107420.

Zhu, W.F., Xu, S.Q., Shao, P.P., Zhang, H., Jia, F., Wu, D.L., Yang, W.J., 1997. Investigation on intake allowance of rare earth-a study on bioeffect of rare earth in South Jiangxi. China Environ. Sci. 17(1). (in Chinese with English abstract)

Zhu, W.F., Xu, S.Q., Zhang, H., Shao, P.P., Wu, D.S., Yang, W.J., 1996. Investigation of children intelligence quotient in REE mining area: bio-effect study of REE mining area of South Jiangxi. Chin. Sci. Bull. 41, 914-916.

Zhu, X.X., Gao, A.G., Lin, J.J., Jian, X., Yang, Y.F., Zhang, Y.P., Hou, Y.T., Gong, S.B., 2018. Seasonal and spatialvariations in rare earth elements and yttrium of

dissolved load in the middle, lowerreaches and estuary of the Minjiang River, southeastern China. J. Oceanol. Limnol. 36 (3), 700-716.

Zhuang, M., Zhao, J., Li, S., Liu, D., Wang, K., Xiao, P., Yu, L., Jiang, Y., Song, J., Zhou, J., 2017. Concentrations and health risk assessment of rare earth elements in vegetables from mining area in Shandong, China. Chemosphere 168, 578-582.

Figure and table captions

Figure 1: (a) Study area and sampling locations; (b) distribution of aquifer systems; and (c) groundwater level contours and flow directions (modified from Zhan et al. (2016)).

Figure 2: Box diagram of pH (a), TDS (b), and OPR (c) in water samples (GW: groundwater; SW: surface water).

Figure 3: (a) Piper plot for water samples, and (b) plot of δD and $\delta^{18}O$ in water samples (GW: groundwater; SW: surface water; WMWL: world meteoric water line; LMWL: local meteoric water line).

Figure 4: Concentrations of REE in water samples.

Figure 5: Upper Continental Crust (UCC)-normalized REE patterns for water samples.

Figure 6: Modelling results of representative REE (Nd, Eu and Yb) speciation in groundwater (a, b, and c) and surface water (d, e, and f)

Figure 7: A comparison of UCC-normalized REE patterns with those of different other major rivers including Mississippi, Amazon, Indus, Ohio, YangZe, Yellow, and some major rivers in southern China (i.e., Pearl River, Xijang, Minjiang, and Jiulongjiang)

Figure 8: Relationship between anthropogenic Gd (Gd_{anth}) concentrations and total REE (ΣREE) (a), Pb (b), Co (c), and Ni (d) concentrations.

Figure 9: Hazard quotient (HQ) of Gd (a) and La (b) in groundwater and surface water for four population groups (i.e., infants, children, adult males, and adult females)

Figure 10: Spatial distribution of HQ_{Gd} in groundwater ((a): infants; (b): children; (c):

adult males; (d): adult females)

1169

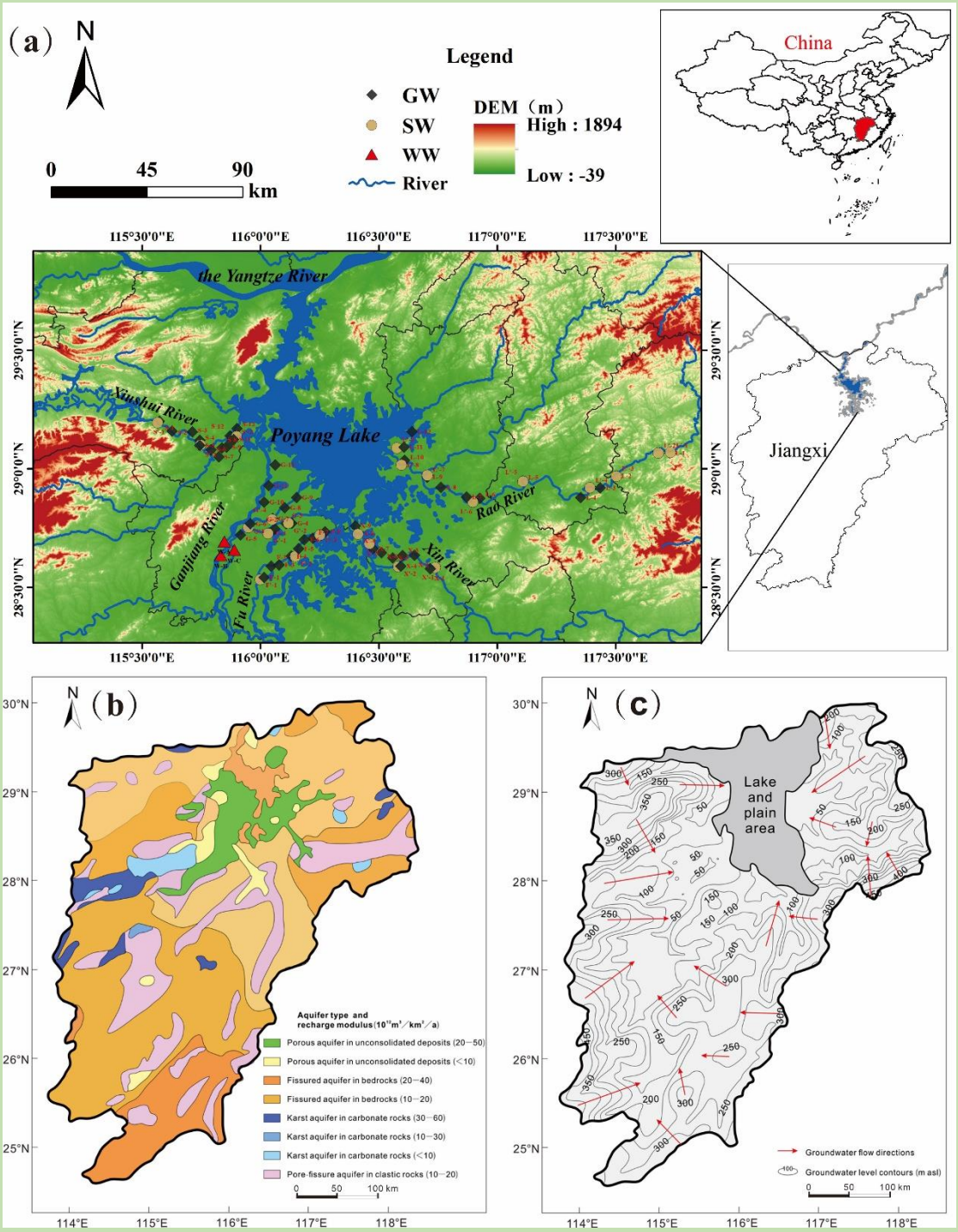

1170

1171 Fig. 1

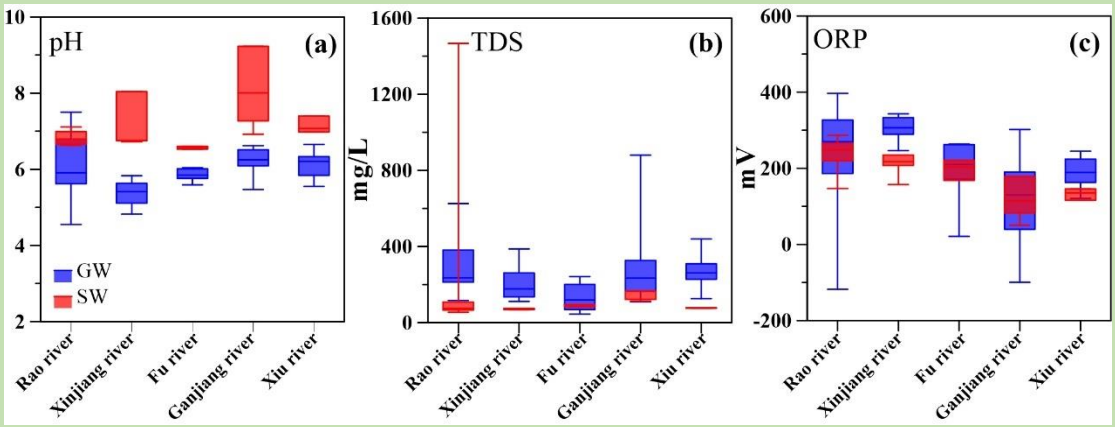

1172

1173 Fig. 2

1174

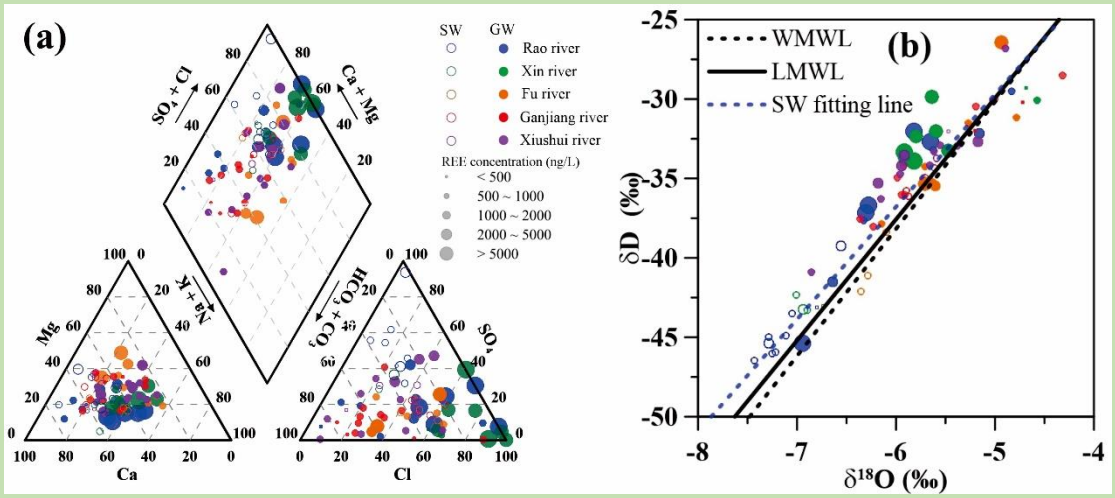

1175

1176 Fig. 3

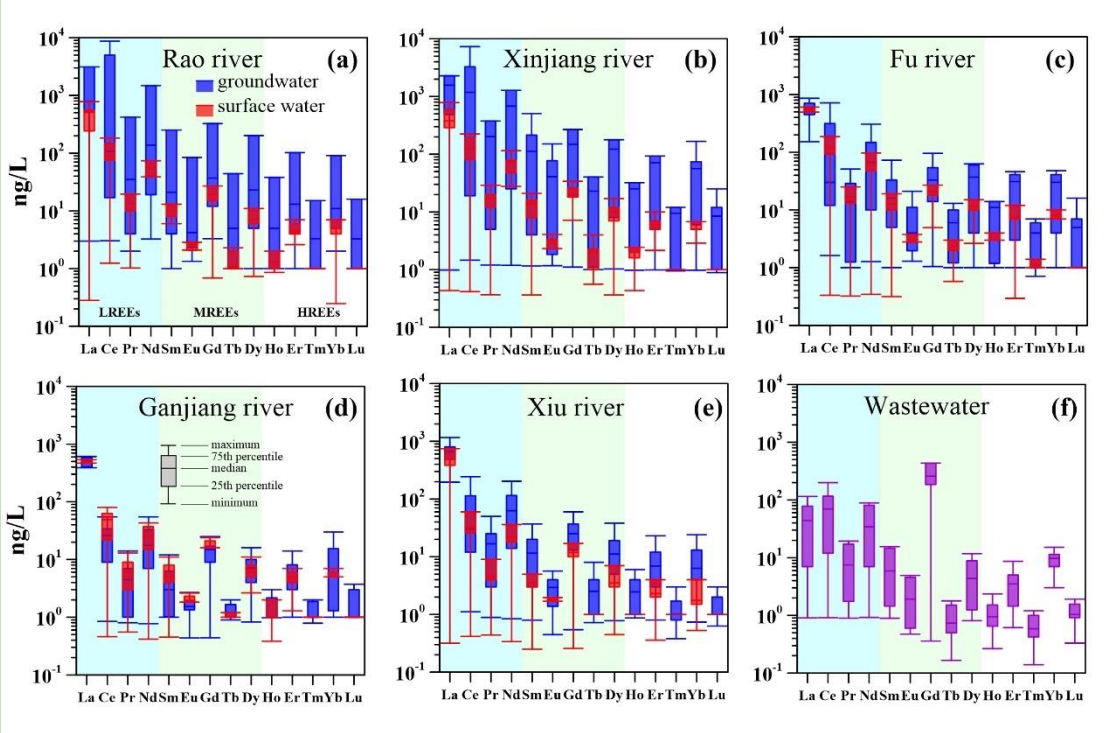
Rao river
(a)
groundwater
surface water
ng/L
LREEs
MREEs
HREEs
Xinjiang river
(b)
Fu river
(c)
Ganjiang river
(d)
maximum
75th percentile
median
25th percentile
minimum
Xiu river
(e)
Wastewater
(f)
La Ce Pr Nd Sm Eu Gd Tb Dy Ho Er Tm Yb Lu

Fig. 4

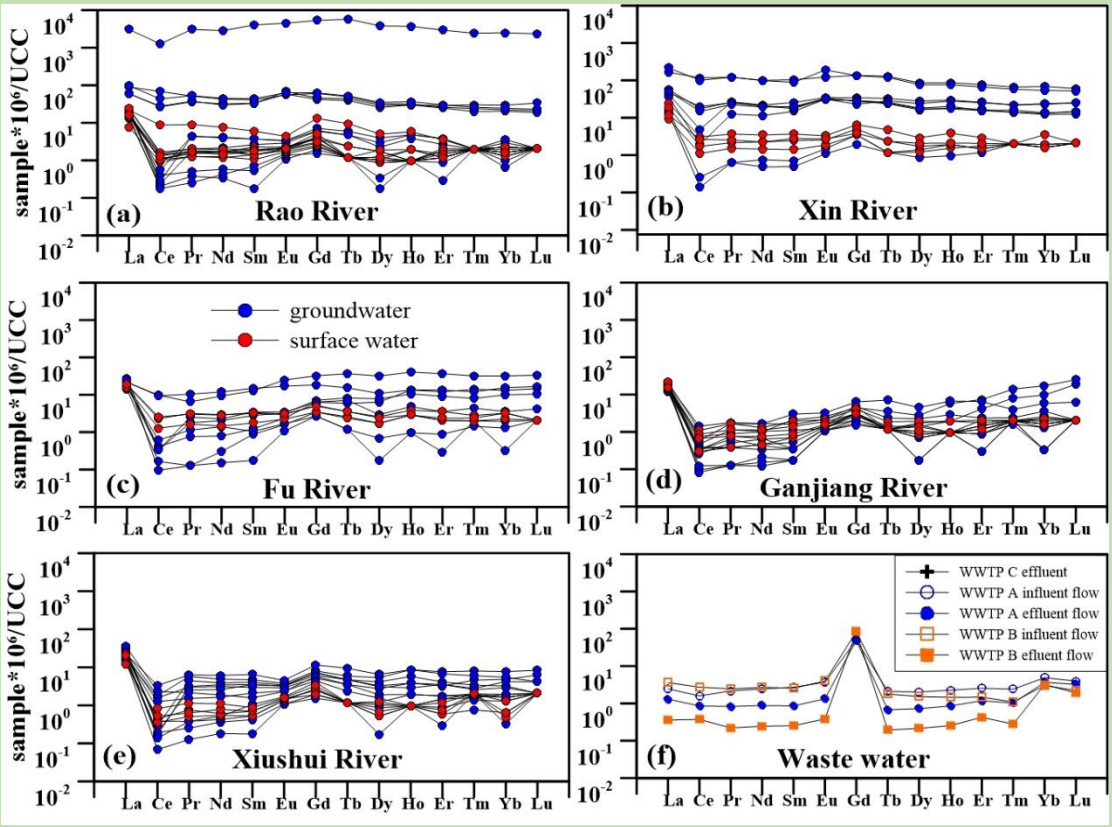
sample*10⁶/UCC
(a) Rao River
(b) Xin River
groundwater
surface water
(c) Fu River
(d) Ganjiang River
(e) Xiushui River
(f) Waste water
WWTP C effluent
WWTP A influent flow
WWTP A effluent flow
WWTP B influent flow
WWTP B efluent flow
La Ce Pr Nd Sm Eu Gd Tb Dy Ho Er Tm Yb Lu

Fig. 5

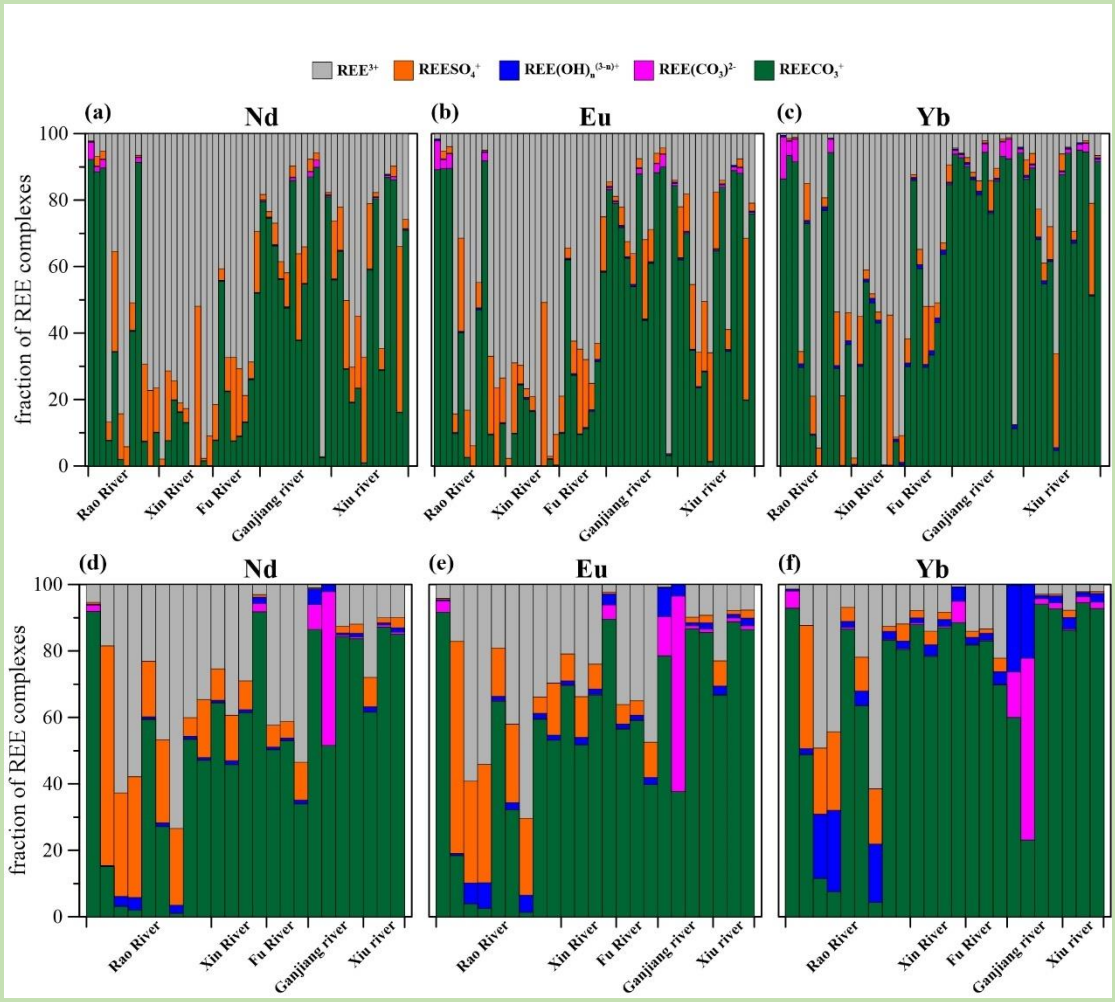
REE3+
REESO4+
REE(OH)n(3-n)+
REE(CO3)2-
REECO3+
(a) Nd
(b) Eu
(c) Yb
(d) Nd
(e) Eu
(f) Yb
fraction of REE complexes
Rao River
Xin River
Fu River
Ganjiang river
Xiu river

Fig. 6

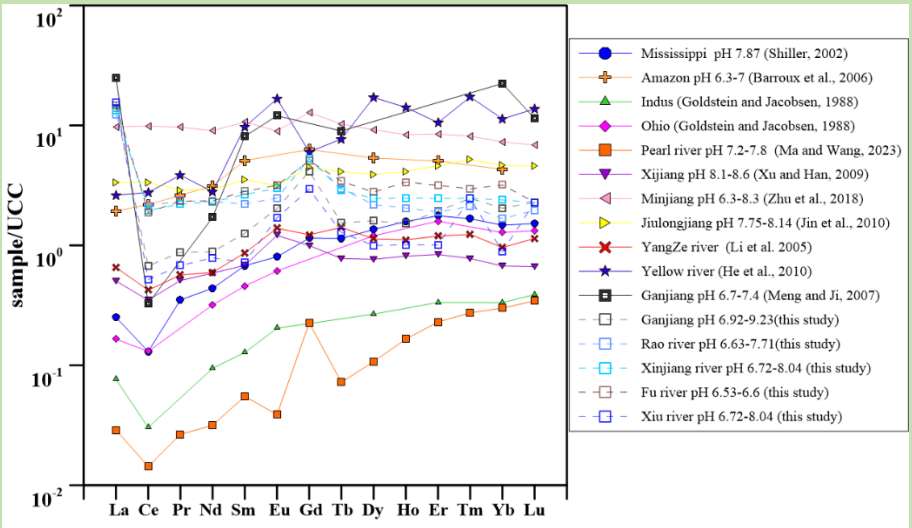
sample/UCC
La Ce Pr Nd Sm Eu Gd Tb Dy Ho Er Tm Yb Lu
Mississippi pH 7.87 (Shiller, 2002)
Amazon pH 6.3-7 (Barroux et al., 2006)
Indus (Goldstein and Jacobsen, 1988)
Ohio (Goldstein and Jacobsen, 1988)
Pearl river pH 7.2-7.8 (Ma and Wang, 2023)
Xijiang pH 8.1-8.6 (Xu and Han, 2009)
Minjiang pH 6.3-8.3 (Zhu et al., 2018)
Jiulongjiang pH 7.75-8.14 (Jin et al., 2010)
YangZe river (Li et al. 2005)
Yellow river (He et al., 2010)
Ganjiang pH 6.7-7.4 (Meng and Ji, 2007)
Ganjiang pH 6.92-9.23(this study)
Rao river pH 6.63-7.71(this study)
Xinjiang river pH 6.72-8.04 (this study)
Fu river pH 6.53-6.6 (this study)
Xiu river pH 6.72-8.04 (this study)

Fig. 7

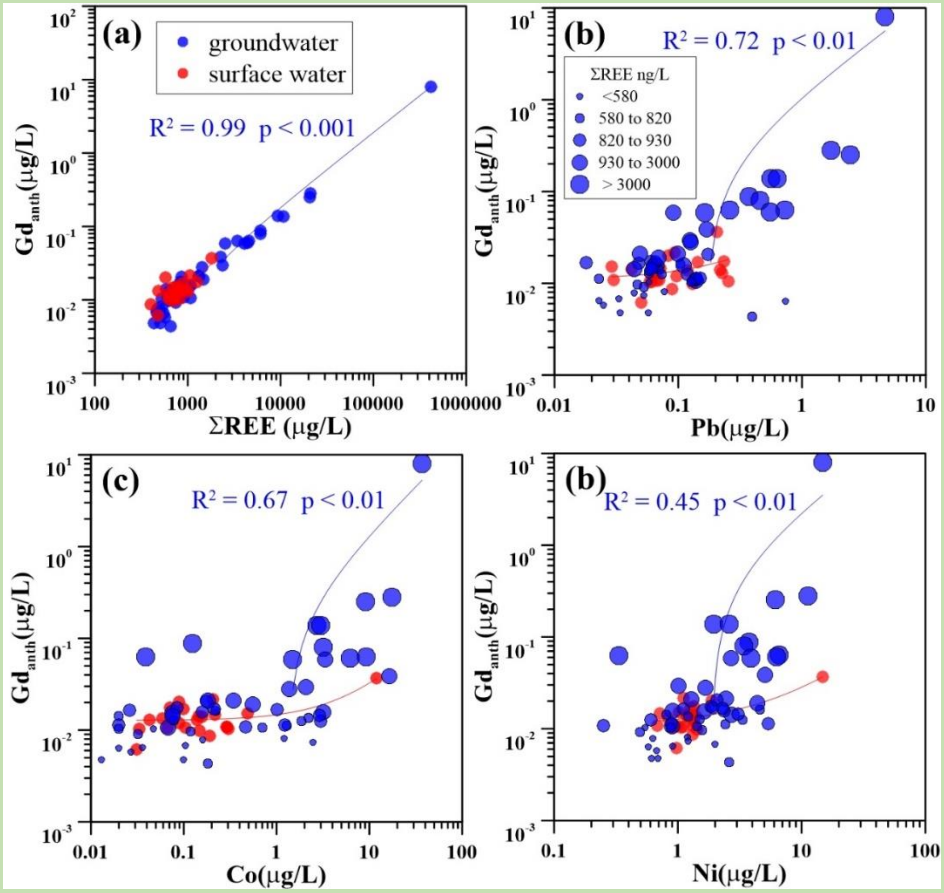
(a)
groundwater
surface water
R² = 0.99 p < 0.001
Gd_anth(μg/L)
ΣREE (μg/L)
(b)
R² = 0.72 p < 0.01
ΣREE ng/L
<580
580 to 820
820 to 930
930 to 3000
> 3000
Pb(μg/L)
(c)
R² = 0.67 p < 0.01
Co(μg/L)
(b)
R² = 0.45 p < 0.01
Ni(μg/L)

Fig. 8

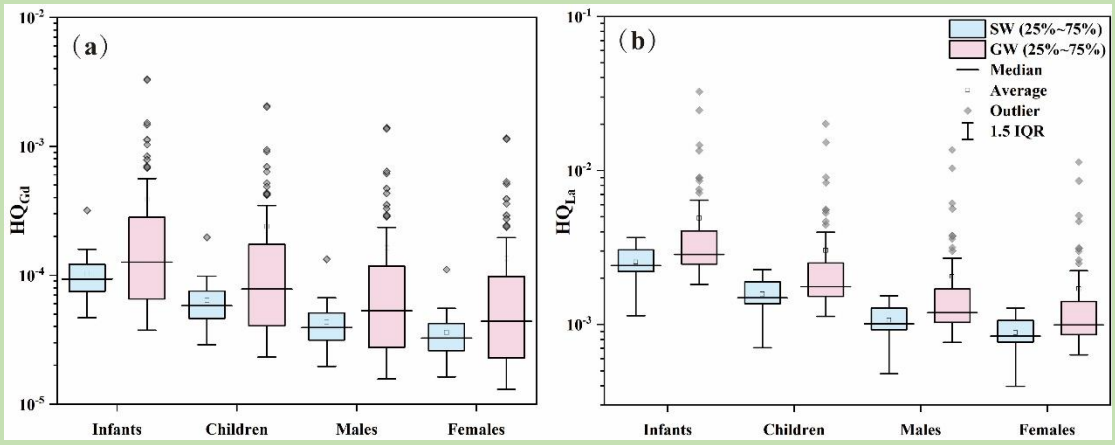
(a)
HQ_Gd
Infants
Children
Males
Females
(b)
HQ_La
SW (25%~75%)
GW (25%~75%)
Median
Average
Outlier
1.5 IQR

Fig. 9

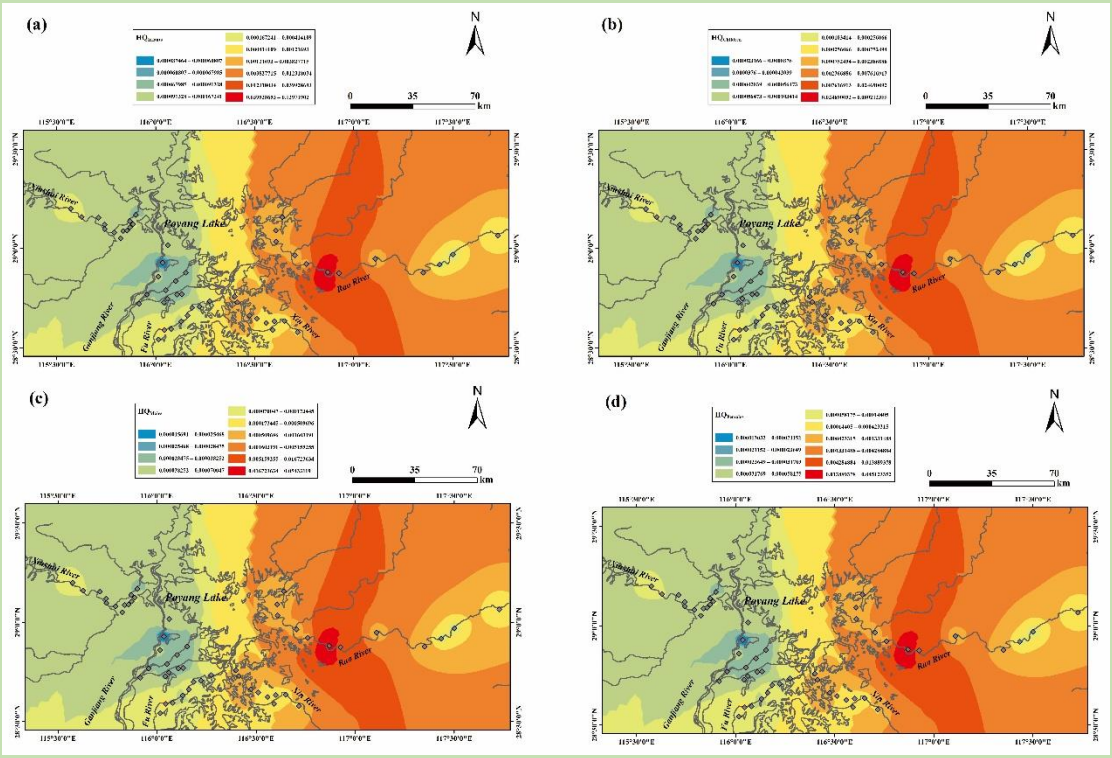
(a)
(b)
(c)
(d)
N
0 35 70
km
Poyang Lake
Xiushui River
Ganjiang River
Fu River
Xin River
Rao River

Fig. 10